applied sciences

Review

Hydrogen Explosion Venting in Confined Spaces: A Review

Juan Pous Cabello [1,2], Álvaro Ramírez-Gómez [2,3,*], Isabel Amez [1,2], Blanca Castells [1,2], David León [1,2], Vanesa Valiño [1,2], Natalia Vázquez [2] and David Bolonio [1,2,*]

[1] Escuela Técnica Superior de Ingenieros de Minas y Energía, Universidad Politécnica de Madrid (UPM), 28003 Madrid, Spain; j.pous@upm.es (J.P.C.); b.castells@upm.es (B.C.); david.leon.ruiz@upm.es (D.L.); vanesa.valino@upm.es (V.V.)

[2] Laboratorio Oficial J.M. Madariaga (LOM)—Centro TECMINERGY, Universidad Politécnica de Madrid (UPM), 28906 Madrid, Spain; natalia.vvinuela@upm.es

[3] Escuela Técnica Superior de Ingeniería y Diseño Industrial, Universidad Politécnica de Madrid (UPM), 28012 Madrid, Spain

* Correspondence: alvaro.ramirez@upm.es (Á.R.-G.); david.bolonio@upm.es (D.B.)

Abstract

Explosion venting is widely used to limit overpressure in confined systems, although its effectiveness depends on complex interactions between combustion, flow, geometry and external conditions. This review examines the phenomenology of vented hydrogen explosions, the main parameters governing their severity, recent experimental and numerical advances, and current design standards. The literature shows that hydrogen concentration, ignition position, vent characteristics, congestion, enclosure geometry and scale affect not only the maximum overpressure, but also the sequence and physical origin of the pressure peaks. Experimental studies highlight the importance of external cloud combustion, flame-acoustic coupling and obstacle-induced turbulence, while CFD models can reproduce overall pressure and flame-propagation trends but remain sensitive to modelling assumptions and validation conditions. Existing standards, particularly EN 14994:2007 and NFPA 68:2023, provide a valuable basis for preliminary design and engineering practice, although additional assessment may be required for highly reactive mixtures, congested layouts and non-standard geometries. Further large-scale testing, benchmark validation and integrated experimental-numerical approaches are needed to improve the reliability of explosion-venting design for hydrogen applications.

Keywords: hydrogen; hydrogen safety; explosion venting; vented deflagration; confined enclosures; explosion protection; industrial safety

Academic Editor: Matt Oehlschlaeger

Received: 19 June 2026
Revised: 9 July 2026
Accepted: 10 July 2026
Published: 14 July 2026

1. Introduction

Transitioning to a decarbonised energy system is one of the key technological, economic and social challenges of the 21st century [1]. In this context, the Paris Agreement and international energy policies have established the need to achieve climate neutrality and drastically reduce greenhouse gas (GHG) emissions over the coming decades [2,3]. Among the various alternatives proposed to achieve this objective, hydrogen has emerged as one of the energy carriers with the greatest potential due to its ability to store, transport and convert energy from various sources, including intermittent renewables such as solar and wind [4].

As a result, the deployment of hydrogen-based technologies is accelerating significantly worldwide. The EU Hydrogen Strategy set a target of 40 GW of installed electrolysis capacity in the European Union by 2030 [5]. In parallel, several countries have increased their national targets for hydrogen production and integration into strategic industrial and energy sectors [6]. This growth is driving the development of new infrastructure associated with the production, storage, compression, distribution and use of hydrogen in industrial, energy and mobility applications.

However, the large-scale deployment of these technologies poses significant challenges from an industrial safety perspective. Hydrogen has physicochemical and combustion properties that differ significantly from those of conventional fuels, which influence the behaviour of leaks, fires and explosions. Among the most relevant properties are its wide flammability range, extremely low minimum ignition energy and high combustion rate [7,8]. Furthermore, its high diffusivity, low density and high sensitivity to turbulence favour flame acceleration phenomena and the development of severe overpressures in confined or semi-confined spaces. The main physicochemical properties of hydrogen and a comparison with other conventional fuels are summarised in Table 1.

Table 1. A comparison of the properties of H_2 with those of other fuels [7].

Fuel	LHV [1] (MJ/kg)	HHV [2] (MJ/kg)	Gas/Vapour Density (kg/m^3)	Liquid Density (kg/m^3)	Boiling Point (K)	Flame Temp. (K)	AIT [3] (K)	Stoich. Ratio (Air/Fuel)	LFL [4]/UFL [5] (%vol)	MIE [6] (mJ)	Diffusion Coef. in Air (cm^2/s)
Hydrogen	120	142	0.09	70.8	20.3	2480	833	34.3	4.0–75.0	0.02	0.61
Propane	46	50	1.83	493	231	2198	723	15.6	2.1–9.5	0.30	0.10
Methanol	18	23	1.30	792	338	2143	733	6.5	6.7–36	0.14	0.17
Methane	50	55	0.72	420	112	2187	813	17.2	5.0–15.0	0.28	0.22
Diesel *	43	45	6.0–7.0	850	580	2200	453–593	14.5	0.6–5.5	0.20–0.30	0.04–0.06
Petrol *	44	47	3.6–4.8	720	383	2250	533–733	14.6	1.3–7.1	0.25–0.35	0.05–0.08

[1] Lower Heating Value. [2] Higher Heating Value. [3] Auto-ignition temperature. [4] Lower Flammable Limit. [5] Upper Flammable Limit. [6] Minimum Ignition Energy. * Non-pure fuel: a commercial mixture of hydrocarbons. The values are typical ranges and may vary depending on composition, temperature, pressure and regulatory specifications.

The practical significance of these risks is reflected in historical records of hydrogen-related accidents and incidents. The HIAD 2.2 (Hydrogen Incidents and Accidents Database), maintained by the European Commission's Joint Research Centre (JRC), compiles 1142 hydrogen-related events recorded up to 31 December 2025 [9]. Within this set of events, consequences associated with explosions appear in more than 460 cases, whilst fires are present in approximately 430 [9]. Although this database is not designed to compare technologies or establish liability, it is a valuable tool for identifying recurring patterns associated with leaks, accidental ignitions, explosions and safety failures in industrial hydrogen facilities.

Among the various mitigation strategies available, explosion venting is one of the most widely used passive protection measures, due to its relative simplicity of implementation, to limit the consequences of accidental deflagrations in explosive atmospheres. Its main objective is to reduce the overpressure generated during combustion through the controlled discharge of gases to the outside of the protected enclosure, as shown in Figure 1 [10,11]. However, the behaviour of vented hydrogen explosions is highly complex due to the strong interaction between combustion, turbulence, enclosure geometry, internal obstacles and external confinement conditions. Furthermore, the design methodologies set out in current regulations and standards are, in many cases, based on simplified configurations that do not adequately represent the actual conditions present in numerous modern industrial facilities [12].

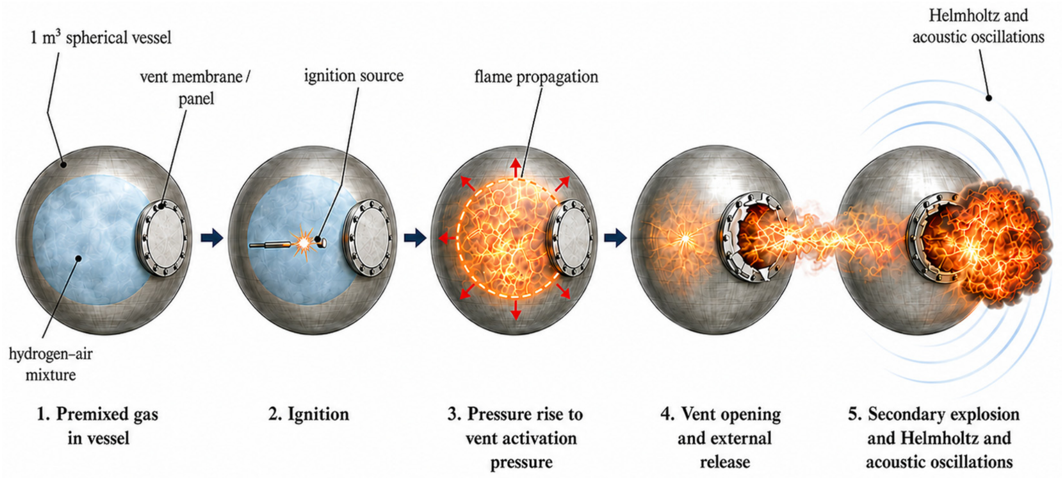

Figure 1. Illustrative example of the venting process.

In this context, this paper reviews the physical and phenomenological foundations of vented hydrogen explosions, the influence of key parameters on explosion severity, recent experimental and numerical developments, and the principal standards and design approaches currently in use. The literature was identified through a targeted search of journal articles, technical reports and standards using combinations of terms such as "hydrogen explosion", "vented deflagration", "explosion venting", "confined enclosure", "vent panel", "pressure relief", "hydrogen–air mixtures", "CFD modelling" and "vent sizing". Priority was given to highly cited studies, recent contributions, experimental campaigns, validated numerical investigations and documents directly relevant to the mechanisms and design issues addressed. The selected references were organised according to the structure of the review, and the main knowledge gaps and future research needs were subsequently identified.

2. Fundamentals and Phenomenology of Vented Hydrogen Explosions

Vented hydrogen explosions in confined spaces are a physically highly complex phenomenon, governed by the interaction between combustion [13], fluid dynamics [14], momentum transfer [15], hydrodynamic instabilities [16] and, in some cases, the structural response of the enclosure [17]. In contrast to a fully confined explosion, in which the pressure evolves primarily due to the expansion of combustion products within a closed volume, a vented explosion involves an additional determining mechanism: the dynamic coupling between the interior of the enclosure and the external environment [18,19].

Venting should not be understood solely as a means of pressure relief, but as a factor that modifies flame propagation, the discharge of unburned mixture, the formation of external flammable clouds, and the sequence of pressure peaks. Consequently, the system's response is not usually defined by a single overpressure peak, but by a series of transients associated with different physical mechanisms [20,21]. This sequential and coupled process explains the dispersion observed in the experimental results and the difficulties of simplified correlations in robustly predicting the dominant pressure peak in different configurations.

2.1. Combustion Regimes

Depending on the flame propagation mechanism and its interaction with the environment, explosions in confined spaces can occur primarily under two regimes: deflagration and detonation. Deflagration is the most common regime in accidental explosions and is characterised by the subsonic propagation of the flame front relative to the unburned mixture. In this case, combustion progresses via molecular transport mechanisms of heat and mass from the reaction zone towards the reactants, whilst the expansion of the combustion gases generates the pressure increase within the enclosure [22].

In hydrogen–air mixtures, deflagration can be particularly severe due to the high combustion rate of hydrogen and its marked sensitivity to turbulence, with resulting pressures potentially ranging from a few bar to around 7–8 bar. Furthermore, in lean mixtures, the low Lewis number favours the early onset of thermodiffusive instabilities, cellular structures and flame front wrinkling, increasing the effective combustion rate even in the absence of high initial turbulence [23–25].

On the other hand, detonation represents a more destructive regime. In this case, the combustion front is coupled to a shock wave and propagates at supersonic speeds, generally in the order of 1500–2000 m/s in hydrogen–air mixtures [22]. The extreme compression associated with the shock wave raises the temperature of the mixture until it ignites, resulting in pressures higher than those of a deflagration. For detonating hydrogen mixtures, pressures can range from 15–20 bar and may increase locally due to wave reflection off walls or obstacles [22].

Between these two extremes, what is known as the deflagration-to-detonation transition (DDT) may occur. This phenomenon is particularly relevant in the case of hydrogen, as the presence of obstacles, partial confinement, pipework, equipment, or elongated geometries can induce turbulence, accelerate the flame and favour the transition to much more violent regimes [26].

The fundamental differences between the two combustion mechanisms are summarised in Table 2.

Table 2. Comparison of key parameters for deflagration and detonation.

Parameter	Deflagration	Detonation
Propagation mechanism	Heat and mass transfer	Coupled shock wave
Pressure front	Weak (1–10 bar)	Strong (>15 bar)
Propagation speed	Subsonic (0.001–100 m/s)	Sonic—supersonic (>1000 m/s)
Reaction zone vs. wavefront	Delayed	Coupled

2.2. Pressure Development

The pressure evolution during a vented hydrogen explosion is one of the key aspects in the design and evaluation of explosion mitigation systems. In this context, it is necessary to distinguish between several characteristic parameters commonly used in the analysis of vented explosions: the maximum explosion pressure (P_{max}), the static venting activation pressure (P_{stat}) and the reduced explosion pressure (P_{red}) [27].

The maximum explosion pressure, P_{max}, corresponds to the maximum overpressure reached in a completely enclosed space under standardised conditions. For stoichiometric hydrogen–air mixtures, this value is typically between 8 and 9 bar [22]. On the other hand, the static activation pressure, P_{stat}, represents the pressure differential at which the venting device opens or breaks mechanically, initiating pressure relief. Finally, the reduced explosion pressure, P_{red}, corresponds to the maximum overpressure recorded once the venting system has been activated, constituting the main design parameter from a structural point of view [27].

Figure 2 graphically illustrates the relationship between P_{max}, P_{red} and P_{stat}.

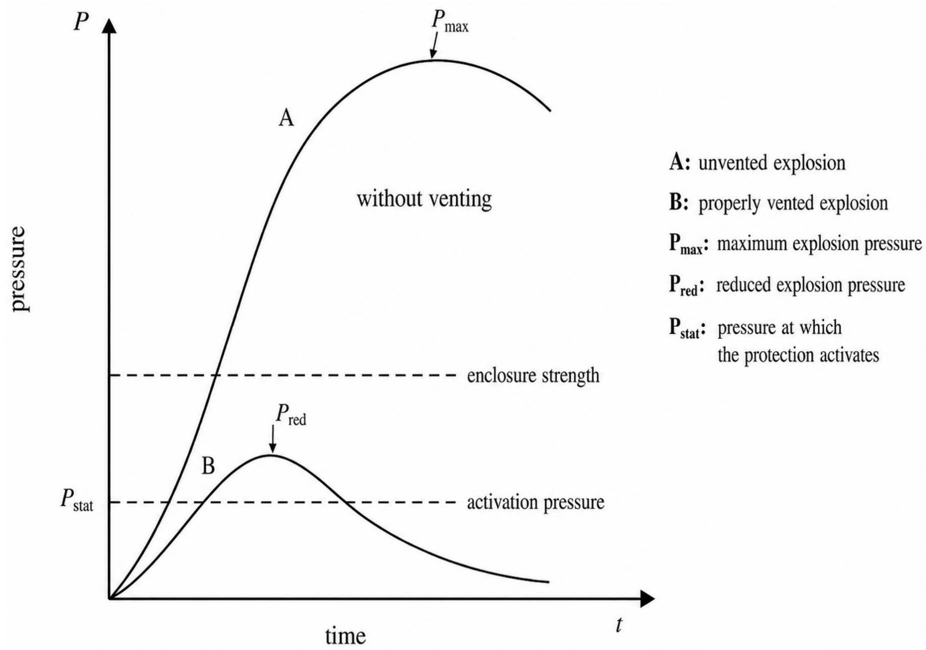

Figure 2. Graphical representation of P_{max}, P_{red} and P_{stat}.

Once these characteristic pressure parameters have been defined, it should be noted that the pressure development in a vented hydrogen explosion cannot be described solely by P_{red}. Although this parameter is fundamental to the design, the temporal evolution of the pressure responds to a succession of internal and external phenomena that can generate several distinct peaks [20,28,29].

Following ignition, the flame initially propagates within the enclosure with an approximately spherical or hemispherical geometry, depending on the ignition position and the proximity of the walls [30]. During this phase, the expansion of the combustion products causes a progressive increase in internal pressure. When P_{stat} is reached, the panel opens [27]. This event introduces an initial transient associated with the activation of the venting itself, which is frequently designated in the literature as P_v or P_{burst} [31].

From that moment on, the system ceases to behave as a practically closed volume and the exchange of mass and energy with the outside begins. The opening of the vent generates an outflow driven by the pressure difference between the enclosure and the surrounding environment. Its intensity depends, among other factors, on the vent area, the activation pressure, the inertia of the panel and the vent geometry [32–35]. Depending on the position of the flame front at the moment of opening, the expelled flow may consist of hot products, fresh unburned mixture, or a combination of both [36].

When a significant fraction of the unburned mixture is expelled to the outside, a flammable cloud may form in front of the vent. Upon reaching the opening, the flame front may ignite this cloud, producing a secondary external explosion, commonly identified as P_{ext} [29,37]. This phenomenon may become the dominant mechanism of overpressure or, at the very least, influence the subsequent evolution of the internal pressure.

Following the external explosion, low-frequency oscillations associated with the combined behaviour of the enclosure and vent may occur, typically interpreted as Helmholtz oscillations. In later stages, coupling may also develop between the flame and the acoustic modes of the enclosure, generating higher-frequency oscillations and additional pressure peaks [26,38–40]. Experimental studies have shown that these oscillatory pressure components should not necessarily be treated as secondary effects, since flame-acoustic interaction may generate the highest pressure peak in certain vented deflagration configurations [41]. In the presence of obstacles or internal congestion, flame-obstacle interaction increases the combustion surface area, intensifies turbulence and may give rise to an additional dominant peak, associated with the sudden increase in the effective combustion velocity [42].

From a structural point of view, this multi-peak and oscillatory behaviour means that P_{red} should be interpreted as the envelope of the complete pressure-time history rather than as a quasi-static pressure value. A single peak-load criterion may be acceptable only when the selected design pressure captures all relevant transient and oscillatory contributions and when the protected structure responds essentially in a quasi-static manner. However, for lightweight, deformable, or dynamically sensitive structures, additional indicators such as impulse, pressure duration, frequency content and dynamic amplification should be considered.

This does not necessarily imply that conventional fatigue limits should be incorporated as a universal requirement in vent-sizing calculations, since vented deflagrations are short-duration accidental events. Nevertheless, when high-amplitude oscillatory loads are expected, pressure-time-based structural assessment or coupled CFD-finite element analysis may be required to evaluate plastic deformation, local buckling, accumulated damage, or ultimate limit states [43].

Therefore, the maximum pressure recorded during a vented explosion may be associated with different mechanisms depending on the system configuration. In some cases, the external explosion dominates; in others, delayed internal combustion, acoustic oscillations, or interaction with obstacles. This multi-peak structure constitutes one of the most characteristic features of the phenomenology of vented hydrogen explosions and justifies the need to analyse the complete temporal evolution of the pressure, and not merely the maximum value of P_{red}.

2.3. Internal-External Interaction Mechanisms

One of the most characteristic aspects of vented explosions is the coupling between the processes occurring inside the enclosure and those taking place outside. The external explosion is not an independent phenomenon, but rather a phase of the process capable of influencing the internal dynamics of the system [16,29,37,44].

In general terms, the process can be summarised as follows: (1) following the opening of the vent, the overpressure draws the flammable mixture outwards; (2) when the flame reaches the vent opening, this mixture ignites; (3) the external combustion generates overpressure at the vent and (4) this overpressure reduces the pressure gradient between the interior and the exterior. As a result, the efficiency of the venting may decrease significantly and the vent may even become temporarily blocked, leading to a further increase in pressure within the enclosure [45,46].

This mechanism, commonly known as the 'blocking effect', explains why an increase in the vent area does not always result in a proportional reduction in internal pressure. In certain configurations, a larger vent may facilitate the expulsion of a greater quantity of unburned mixture, intensifying the external explosion and increasing its influence on the internal pressure [47,48]. Similarly, ignition at positions distant from the vent may favour a longer flame path, a more intense discharge of fresh mixture and a more severe external explosion [49].

Hydrodynamic instabilities also play a significant role in this coupling. Rayleigh–Taylor instability occurs when the less dense combustion products are accelerated towards the denser unburned mixture, increasing the wrinkling of the flame front and its effective surface area [15,16,25,50]. For its part, the Kelvin–Helmholtz instability develops in regions of high shear, such as the boundary layers of the exhaust jet or the interaction zones between the flame and the vortices generated by obstacles, increasing mixing and local turbulence [51,52].

From a physical point of view, the problem cannot be treated as an internal deflagration with an open and fixed boundary condition. The boundary represented by the venting evolves dynamically during the process and is conditioned by the phenomena that the system itself generates externally. Therefore, an adequate description of vented hydrogen explosions requires explicit consideration of the internal-external coupling, the morphological evolution of the flame, the formation of external clouds, the generation of instabilities, and the possible occurrence of multiple pressure peaks.

Figure 3 schematically summarises the characteristic sequence of events and pressure transients observed during a vented hydrogen explosion.

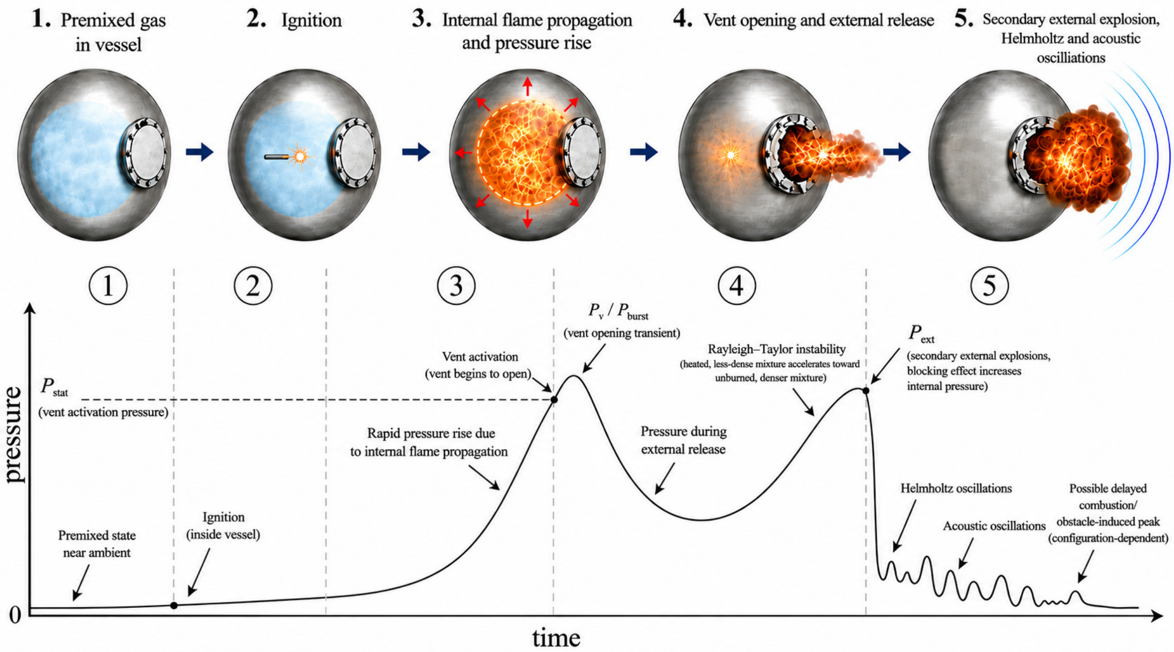

Figure 3. Schematic sequence of pressure transients during a vented hydrogen explosion in a confined enclosure.

3. Influence of Key Parameters on Explosion Severity

As previously discussed, the severity of a vented hydrogen explosion cannot be attributed to a single dominant parameter, but rather results from the non-linear interaction between multiple physicochemical, geometric and operational variables [20]. Although the literature frequently identifies factors such as hydrogen concentration [14], ignition position [53], vent size [31], activation pressure [33], internal congestion [42] or enclosure geometry [13], it also highlights that the influence of each of these factors depends heavily on the rest of the system and on the dominant physical mechanism during each phase of the explosion.

In the case of hydrogen, this multiple dependence is particularly pronounced due to its high combustion rate, high diffusivity and sensitivity to flame instabilities. Consequently, parameters that may have a secondary influence on other fuels come to play a decisive role in the evolution of the explosion. Furthermore, numerous studies have shown that these factors not only modify the maximum overpressure value but also the sequence of peaks, the flame acceleration, the intensity of the external explosion and the spatial distribution of dynamic loads.

3.1. H_2 Concentration and Mixture Reactivity

Hydrogen concentration is one of the most influential parameters governing the severity of a vented explosion, as it directly affects the laminar burning velocity, the overall reactivity of the mixture and the amount of chemical energy released during combustion [25,28,32,38,54–60]. Experimental results consistently show that the explosion overpressure increases as the hydrogen–air mixture approaches stoichiometric conditions. As illustrated in Figure 4 for different initial pressures, the highest pressure values are generally obtained at hydrogen concentrations close to 30% vol [11,44,46,59].

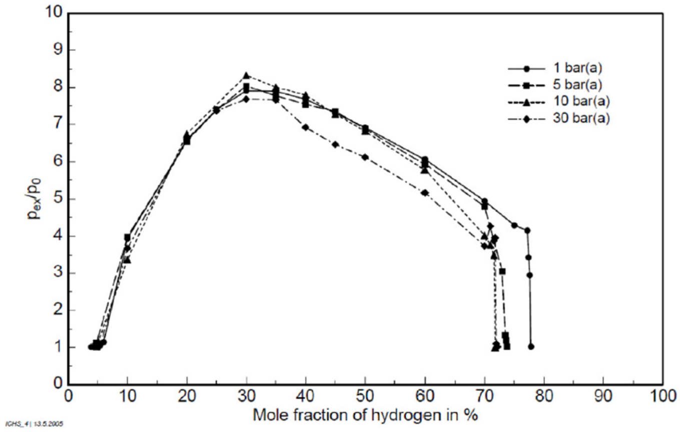

Figure 4. Explosion pressures of hydrogen–air mixtures at 20 °C for different initial pressures of 1, 5, 10 and 30 bar(a). Reproduced from [59]. License: CC-BY.

However, hydrogen concentration affects not only the maximum overpressure, but also the timing, sequence and relative importance of the characteristic pressure peaks generated during vented explosions. Figure 5 combines centrally ignited hydrogen–air explosion tests reported at two markedly different scales: a 1 m^3 enclosure and a 40 ft ISO container [55,60]. In both configurations, P_1 corresponds to the vent opening, P_2 to the external explosion, and P_3 to the subsequent pressure oscillations and flame-acoustic coupling.

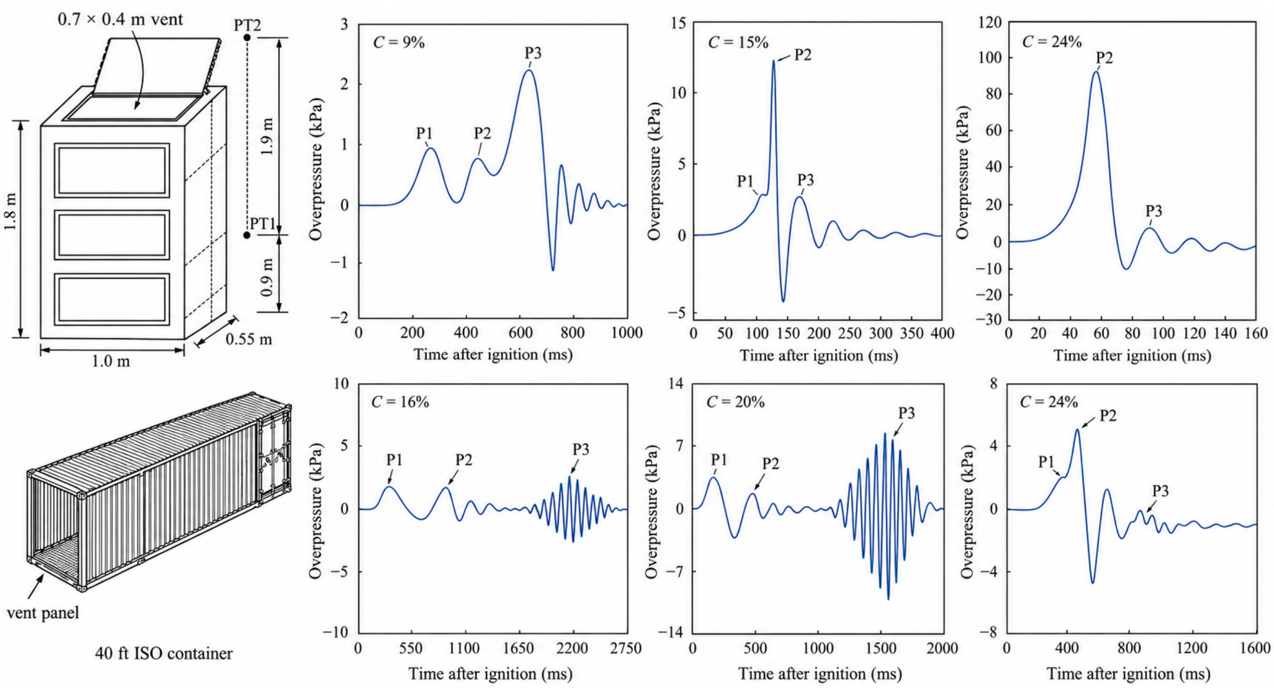

Figure 5. Characteristic pressure histories of centrally ignited vented hydrogen–air explosions at different concentrations and experimental scales: a 1 m^3 enclosure and a 40 ft ISO container. Adapted from [55,60].

The comparison shows a clear concentration-dependent change in peak dominance. In the 1 m^3 enclosure, the leanest mixture considered (C = 9%) is dominated by the oscillatory stage (P_3), whereas at (C = 15%) and especially at (C = 24%), the external-explosion peak (P_2) becomes increasingly pronounced. A comparable tendency is observed in the 40 ft ISO container, where increasing concentration strengthens both the early pressure peaks and the subsequent oscillatory response. Although the absolute pressures and characteristic times differ because of the different enclosure volumes, geometries and venting arrangements, both experimental series confirm that hydrogen concentration controls the sequence and relative contribution of vent opening, external combustion and oscillatory phenomena.

In addition to its effect on pressure generation, hydrogen exhibits distinctive behaviour in lean mixtures because of its low Lewis number ($Le < 1$). Under these conditions, preferential diffusion promotes thermodiffusive instabilities, cellular flame structures and premature wrinkling of the flame front [20,24,28,61,62]. These effects increase the effective flame surface area and may result in combustion velocities substantially higher than those predicted by classical laminar-flame models.

In practical scenarios, mixture stratification introduces an additional level of complexity. Owing to its low density and high buoyancy, hydrogen may form pronounced vertical concentration gradients, with richer and more reactive mixtures accumulating in the upper regions of an enclosure. Consequently, the homogeneous stoichiometric mixture should be understood as a useful reference scenario for preliminary assessments, but not necessarily as the only realistic worst-case condition for vented hydrogen explosions. In stratified releases, the upper layer may govern the explosion severity because it can contain the maximum local hydrogen concentration, while the lower part of the enclosure remains leaner or even outside the flammable range [63,64]. This is particularly relevant for roof vents or elevated side vents, where the discharged cloud may be richer than the nominal average composition and may, therefore, generate a different external explosion hazard. Safety assessment should, therefore, consider both homogeneous reference mixtures and physically realistic stratified scenarios derived from credible leak and ventilation conditions.

3.2. Ignition Position

The ignition position determines the flame propagation distance before the flame reaches the vent, thereby affecting flame acceleration, the amount of unburned mixture expelled from the enclosure, and the coupling between internal combustion and external venting phenomena [24,40,49,65].

In general, ignition at a location remote from the vent produces higher internal overpressures than ignition close to the opening [14,35,49,66]. A longer propagation path allows the flame front to accelerate and displace a larger volume of unburned mixture towards the vent. The subsequent discharge may form a larger and more reactive external flammable cloud, whose ignition can intensify the external explosion and influence the internal pressure evolution.

Conversely, ignition close to the vent generally results in lower internal overpressures because the flame reaches the opening earlier, part of the combustion products is discharged more rapidly, and less unburned mixture remains confined within the enclosure [35,66,67]. Nevertheless, this trend is not universal. Depending on the enclosure geometry, vent size and hydrogen concentration, central ignition may produce pressure peaks comparable to, or even higher than, those associated with ignition farther from the vent [35,53].

Figure 6 presents the experimental configuration considered in [53], including the top, central and bottom ignition locations, together with the corresponding maximum overpressures measured at different hydrogen concentrations. The results show that the influence of ignition position becomes increasingly pronounced as the hydrogen concentration rises.

Top ignition consistently produces the lowest peak overpressures, whereas bottom ignition generally generates the highest values. The difference is particularly marked at 25% vol H_2, for which the maximum overpressure increases from approximately 0.08 bar for top ignition to 0.42 bar for central and 0.51 bar for bottom ignition.

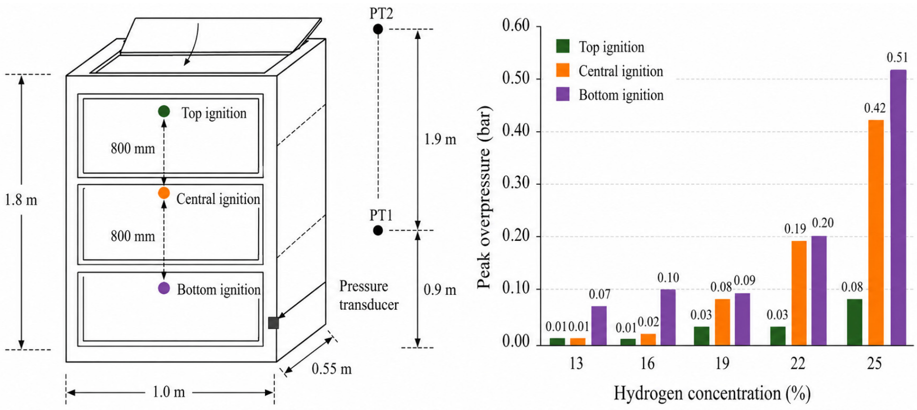

Figure 6. Experimental configuration, ignition locations and maximum overpressure as a function of hydrogen concentration. Adapted from [53].

The influence of the ignition position is not limited to the maximum internal overpressure. It also affects the amount of unburned mixture discharged through the vent, the intensity of the external explosion (P_{ext}), the morphology and length of the emerging flame, and the timing and relative magnitude of the characteristic pressure peaks [14,67]. Ignition location should, therefore, be considered together with hydrogen concentration, vent geometry and enclosure configuration when assessing the severity of vented hydrogen explosions.

3.3. Venting Parameters

The characteristics of the venting system are among the principal factors governing pressure relief during explosions in confined enclosures [15,21,24,25,31,32,36,56,57,66,68–73]. The most relevant parameters include the vent area (A_v), the nondimensional vent coefficient ($K_v = V^{2/3}/A_v$, where V is the volume of the enclosure), the static activation pressure of the venting device (P_{stat}), and the number, orientation and geometric arrangement of the vents.

In general, increasing the vent area enhances the discharge of combustion products and unburned mixture, thereby tending to reduce the maximum internal overpressure. Nevertheless, the relationship between A_v and the reduced explosion pressure is not strictly linear. A larger opening may promote the discharge of a greater quantity of unburned mixture, resulting in the formation of a more extensive external flammable cloud. Its subsequent ignition can intensify the external explosion, modify the pressure difference across the vent and alter the dominant pressure-generation mechanism [48]. Consequently, increasing the vent area does not necessarily produce a proportional reduction in the overall severity of the event.

The vent coefficient (K_v) provides a useful means of relating the vent area to the characteristic size of the enclosure. Because K_v increases as the vent area decreases, high values indicate progressively more restricted pressure relief. Experimental investigations with hydrogen–air mixtures have identified marked changes in the pressure response as K_v increases [74]. For relatively large vents, the pressure history is characterised by several distinguishable transient peaks and oscillatory stages. As the opening becomes smaller, venting efficiency decreases, the pressure associated with restricted discharge becomes increasingly dominant and the secondary peaks become less identifiable. Under the most restrictive conditions, the response is governed by a single large pressure maximum.

Table 3 summarises this evolution for selected vent areas investigated in [74]. The results show that the maximum overpressure increases only moderately between (K_v = 5.00) and (K_v = 8.33), but rises substantially for higher values. In particular, reducing the vent area from 0.12 to 0.08 m^2 increases the approximate maximum overpressure from 0.31 to 0.80 bar, whereas a further reduction to 0.04 m^2 produces a maximum of approximately 2.90 bar. These findings illustrate that, once the effective relief capacity becomes insufficient, relatively small reductions in vent area may lead to disproportionately large increases in explosion overpressure.

Table 3. Summary of the pressure response for different vent areas and vent coefficients, based on the experimental results reported in [74].

K_v	A_v (m^2)	Approx. Max. Overpressure (Bar)	Dominant Pressure Behaviour
5.00	0.20	0.16	Multiple transient peaks; the maximum is associated with late flame-acoustic oscillations
8.33	0.12	0.31	Broad pressure plateau caused by reduced venting efficiency, followed by a secondary oscillatory peak
12.50	0.08	0.80	Restricted venting produces a broad dominant pressure maximum; secondary peaks become difficult to distinguish
25.00	0.04	2.90	Insufficient venting produces a single dominant pressure maximum.

The activation pressure of the relief device also has a significant influence on explosion dynamics. A high P_{stat} delays the opening of the vent and allows greater pressure accumulation within the enclosure before relief begins [68]. This delay generally increases the initial pressure transient and may also modify the quantity and momentum of the mixture discharged through the opening. Consequently, the severity of the external explosion and the duration and amplitude of the subsequent Helmholtz oscillations may also be affected.

The geometric configuration of the venting system provides an additional source of variability. Vent orientation determines the direction of discharge, the morphology of the external flame and the spatial distribution of the resulting pressure loads [26,47]. In industrial applications, vent ducts are often required to direct flames and hot gases towards a safe discharge location. Although this is an appropriate protection strategy and is considered in design practice, ducting means that the nominal vent area no longer represents the actual relief capacity of the system. Duct length, hydraulic diameter, bends, roughness and outlet conditions introduce pressure losses and flow inertia, and restrictive configurations may lead to critical or choked-flow conditions [36,72]. Therefore, ducted venting should be assessed using an effective discharge capacity, equivalent vent area, or discharge coefficient, with case-specific evaluation when long ducts, small diameters, multiple bends, or strong acoustic coupling with the enclosure are expected.

3.4. Internal Congestion and Obstacles

Internal congestion is one of the most influential factors in the intensification of hydrogen explosions [10–12,17,31,55,57,64,69,72]. When the flame interacts with obstacles, the flow separates around their surfaces and generates recirculation zones, shear layers and turbulence in their wake. These mechanisms wrinkle and stretch the flame front, increase its effective surface area and accelerate the overall combustion process. As a result, flame propagation becomes faster and the pressure rise within the enclosure may increase substantially.

Experimental and numerical studies have shown that higher blockage ratios and shorter spacing between obstacles can produce marked increases in maximum overpressure [11]. The position of the obstacles relative to the ignition source and the vent is also important because it determines where flame acceleration occurs and how the resulting pressure transients interact with the relief process [42]. Obstacle geometry introduces an additional source of variability by modifying the separation points, wake structure and intensity of the recirculating flow. Figure 7 schematically shows how obstacle geometry modifies the streamline pattern, flame-front deformation and shock-wave structure. Circular obstacles produce smoother flow deviation, whereas square and triangular geometries promote stronger separation, recirculation and flame deformation [39,52].

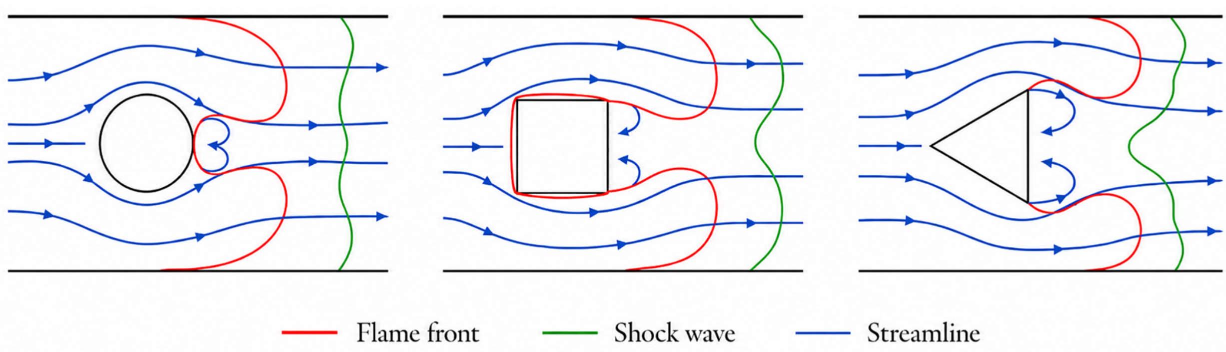

Figure 7. Schematic influence of circular, square and triangular obstacles on the streamline pattern, flame-front deformation and shock-wave structure. Adapted from [52].

Hydrogen is particularly sensitive to these effects because of its high reactivity and the strong coupling between turbulence and flame instabilities. Consequently, components introduced as part of the protection strategy should not automatically be assumed to attenuate combustion, since under some conditions they may produce the opposite effect by acting as turbulence-generating obstacles. For example, metallic meshes and grilles may increase local turbulence, promote flame wrinkling and accelerate combustion rather than suppress it [75]. Therefore, such devices should be included in the congestion assessment unless their suppressive performance has been specifically validated for the relevant hydrogen–air mixture, geometry, flow conditions and expected flame regime. More generally, internal congestion should not be characterised solely through global parameters such as blockage ratio. In early-stage design, this parameter should be complemented by a hierarchical description of congestion, including obstacle shape, size, spacing, orientation, number of obstacle layers along the expected flame path, position relative to the ignition source and vent, and the presence of highly congested regions. A practical approach is to divide the enclosure into congestion zones and evaluate the likely flame path through open volumes, moderately congested areas and critical pipework or equipment regions where flame acceleration is more likely. This simplified description does not replace detailed CFD but provides a more representative basis for preliminary screening and for selecting the configurations that require higher-fidelity assessment.

3.5. External Congestion and Confinement

Obstacles and structures located outside the enclosure can significantly influence the severity of vented explosions [76,77]. Nearby buildings, walls, process equipment, modular units, pipe racks, canopies, or deflection structures may partially restrict the discharge flow, alter the development of the external flame and promote the reflection of pressure waves. These effects can increase the intensity of the external explosion and modify the pressure response inside the enclosure.

This influence is particularly relevant in compact industrial facilities, where the separation distance between adjacent units may be limited. Under these conditions, the vented jet and external combustion products may interact with surrounding structures before they can expand freely. As schematically illustrated in Figure 8, an unconfined environment allows the vented flow, external flame and pressure waves to propagate with relatively little obstruction. By contrast, a nearby wall or structure restricts the discharge, redirects the external flame and promotes the reflection of pressure waves towards the enclosure. The resulting confinement can reduce the effective pressure gradient across the vent, hinder the relief process and increase the dynamic loads transmitted both to the enclosure and to nearby equipment.

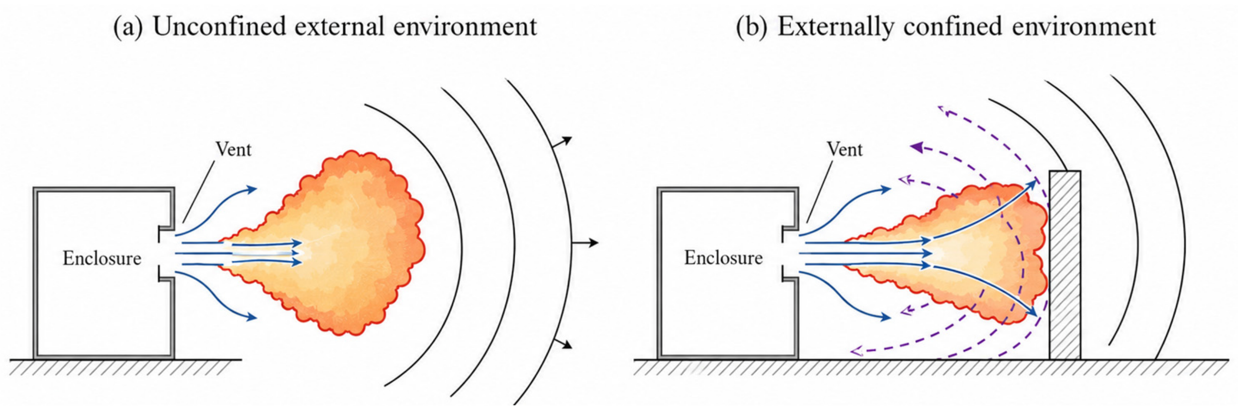

Figure 8. Schematic comparison of vented hydrogen explosions in unconfined and externally confined environments.

This problem becomes more complex in non-isolated hydrogen installations, such as semi-open industrial buildings, hydrogen refuelling stations, electrolyser rooms, compressor shelters, skid-mounted process units and distributed hydrogen energy stations. In these configurations, the enclosure to be protected is rarely surrounded by a fully open external domain. Instead, vent outlets may discharge towards adjacent modules, protective barriers, service corridors, vehicle lanes, equipment skids, ventilation louvres or partially confined service areas. The external region may, therefore, behave as a secondary confinement volume, especially when the vented flame or unburned hydrogen–air cloud is redirected or trapped by surrounding structures. Similar concerns may arise in underground or semi-confined hydrogen storage and handling areas, where access galleries, shafts, retaining walls, or limited ventilation paths can restrict cloud dispersion and increase the potential severity of external combustion.

The engineering consequence is that explosion relief in non-isolated scenarios cannot be assessed only from the internal enclosure geometry and nominal vent area. The surroundings of the vent outlet must also be considered part of the effective venting system. Adjacent facility spacing, vent orientation, external flow paths and the presence of deflection or protective structures determine whether the discharged mixture can expand freely or whether the external cloud combustion may feed back into the enclosure through pressure-wave reflection and vent blockage. External diversion structures may reduce flame impingement on sensitive targets if properly designed, but they may also increase confinement if placed too close to the vent outlet or if they redirect the discharge towards obstacles or partially enclosed regions.

The numerical benchmark reported in [76] supports this behaviour. A comparison between externally confined and unconfined configurations showed that the presence of surrounding structures modified both the magnitude and timing of the principal overpressure peaks, increasing the main peak by approximately 45% (from about 0.055 to 0.08 bar_g).

External confinement also altered the subsequent pressure oscillations, demonstrating that the surrounding geometry influences not only the external pressure field but also the internal pressure evolution.

The preliminary dispersion stage also plays a decisive role in determining the severity of the subsequent explosion [78,79]. Wind speed and direction, leak orientation and the geometry of the surrounding environment affect the volume, concentration and persistence of the flammable cloud formed outside the enclosure. Restricted or poorly ventilated external regions may promote the accumulation of larger hydrogen–air clouds, thereby increasing the potential intensity of an external explosion following ignition. This aspect is particularly important for refuelling stations and other distributed hydrogen facilities, where equipment modules, vehicles, barriers and auxiliary structures can change the local ventilation and confinement conditions around the vent discharge path.

Consequently, vent-outlet safety distances should not be treated as static values defined only during the initial design stage. They should be integrated into plant layout planning and periodically reassessed during the operational life of the facility. Any modification involving adjacent equipment, temporary barriers, protective walls, acoustic screens, weather shelters, maintenance enclosures, vehicle parking areas, new pipework, auxiliary skids, or changes in ventilation openings may alter the external confinement conditions and the effectiveness of explosion relief. Therefore, management-of-change procedures for hydrogen installations should explicitly include the reassessment of vent discharge paths, adjacent facility spacing, external obstruction, possible flame impingement and reflected pressure-wave effects.

Overall, the final severity of a vented hydrogen explosion does not depend solely on the relief system, but also on the dispersion, congestion and confinement conditions present in the external environment.

3.6. Geometry and Scale Effects

Enclosure geometry has a decisive influence on the evolution of vented hydrogen explosions because it affects the available flame-propagation distance, interaction with the walls, turbulence generation, acoustic modes and pressure-relief efficiency [13,66]. Relevant geometric parameters include the enclosure volume, the length-to-diameter ratio (L/D), the overall shape of the enclosure, the vent location and the spatial distribution of internal obstacles.

The influence of the (L/D) ratio depends on the dominant combustion and venting mechanisms. Elongated geometries provide a longer path for flame propagation and may, therefore, favour sustained flame acceleration before the flame reaches the vent. Nevertheless, a greater flame path does not necessarily result in a higher maximum internal overpressure. Compact enclosures may produce more severe internal pressure loads because of stronger confinement, greater interaction between the expanding combustion products and the enclosure walls, and reduced spatial dissipation of the pressure field [19].

Figure 9 presents the experimental setup and the influence of the (L/D) ratio on maximum internal overpressure for hydrogen concentrations between 15 and 50% vol. In both geometries, overpressure increases up to approximately 40% vol H_2 and then decreases, although the compact configuration (L/D = 1) consistently produces higher values than the elongated tube (L/D = 16), reaching about 365 kPa compared with approximately 230 kPa.

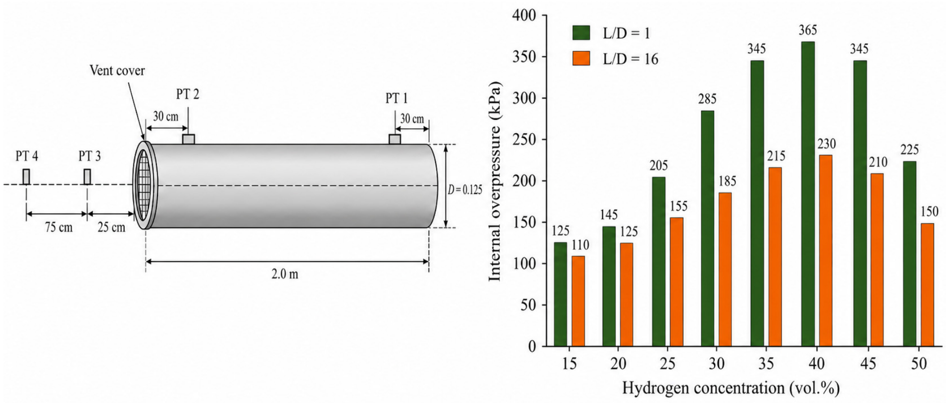

Figure 9. Influence of the L/D ratio on the maximum internal overpressure as a function of hydrogen concentration. Adapted from [19].

In industrial containers and enclosures, additional geometric characteristics, including frontal or top venting, partial or complete wall opening, rigid roofs and non-uniform internal layouts, can substantially modify the sequence of pressure peaks and the structural response of the system [80]. In pipes and elongated enclosures, geometry also affects the balance between internal and external overpressure, and opposing trends may occur as hydrogen concentration and venting conditions vary [19].

Studies conducted at different scales further demonstrate that scaling cannot be addressed solely through enclosure volume. Dimensionless geometric parameters, vent-to-volume ratios, confinement conditions and obstacle distributions can modify the flame regime, the sequence of pressure transients and the dominant pressure-generation mechanism [19]. Consequently, direct extrapolation from small-scale experiments to full-scale industrial configurations remains subject to considerable uncertainty, particularly for hydrogen, because of the strong coupling between turbulence, geometry and flame instabilities.

Finally, Table 4 summarises the principal parameters identified in the literature as influencing the severity of vented hydrogen explosions, including their associated physical mechanisms, their effects on reduced explosion pressure (P_{red}) and flame acceleration, and the main interactions observed between variables.

Table 4. Influence parameters evaluated.

Parameter	Physical Mechanism	Influence on P_{red}	Influence on Flame Acceleration	Main Findings	Interactions	References
H_2 concentration	Increased reaction rate, thermo-diffusive instabilities, enhanced external combustion	P_{red} generally maximised near stoichiometric conditions	Strong increase close to stoichiometry; unstable flames in lean mixtures	Maximum overpressure typically around 30% vol H_2; transition of dominant peak mechanism with concentration	Coupled with turbulence, external explosion and acoustic oscillations	[11,44,46,59,60]
Ignition position	Controls flame travel distance and amount of unburned gas expelled	Rear ignition usually produces highest P_{red}	Longer flame acceleration path for back-wall ignition	Back-wall ignition intensifies P_{ext}; near-vent ignition reduces internal pressure	Strong interaction with vent area, geometry and concentration	[14,35,49,53,67]
Vent area (A_v)/K_v	Governs discharge capacity and external cloud formation	Larger A_v generally reduces P_{red}, but not linearly	Large vents may intensify external flame acceleration	Transition in dominant peaks observed around critical K_v values	Coupled with P_{ext}, choked venting and vent orientation	[47,48,74]

Table 4. *Cont.*

Parameter	Physical Mechanism	Influence on P_{red}	Influence on Flame Acceleration	Main Findings	Interactions	References
Vent opening pressure (P_{stat})	Delays vent activation and modifies initial discharge energy	Higher P_{stat} increases initial pressure peak	Can intensify external combustion due to energetic gas release	Strong influence on first pressure transient and Helmholtz oscillations	Coupled with vent inertia and external explosion	[33,68]
Internal obstacles/congestion	Turbulence generation, flame folding and increase in flame surface area	Significant increase in P_{red}, potentially several-fold	Strong enhancement of flame acceleration	Obstacle geometry and spacing critically affect combustion regime	Coupled with DDT risk, acoustic oscillations and turbulence	[11,39,42,52,57]
External congestion/confinement	Reflection of pressure waves and restriction of vent discharge	Can increase internal P_{red} by reducing venting efficiency	Enhances external flame acceleration and pressure wave amplification	Narrow passages and nearby structures intensify external loads	Coupled with P_{ext} and vent orientation	[76,78,79]
Geometry (L/D)	Controls flame path length, confinement and acoustic modes	Geometry-dependent; compact and elongated enclosures may dominate depending on regime	Long geometries favour sustained flame acceleration	L/D modifies balance between internal and external pressure peaks	Coupled with ignition position, obstacles and vent location	[19,26,80]
Mixture stratification	Non-uniform concentration distribution due to buoyancy	Local rich regions may dominate P_{red}	Localised acceleration in high-reactivity regions	Explosion severity governed by local concentration peaks rather than average	Coupled with leak dynamics and confinement	[11,47,63,64,81]
Vent inertia	Delayed vent deployment and transient pressure accumulation	Higher inertia may increase early pressure peaks	Can delay flame relief and intensify discharge jet	Influences timing of P_{stat} and oscillatory behaviour	Coupled with P_{stat} and vent geometry	[14,34,60]
Number of vents	Modifies flow distribution and external combustion sequence	Multiple vents may reduce local pressure but generate additional transients	Alters flame propagation symmetry	Multiple external peaks observed in multi-vent configurations	Coupled with vent orientation and enclosure geometry	[36,47]
Initial turbulence	Enhances mixing and flame wrinkling	Increased P_{red} due to faster combustion	Strong increase in turbulent flame speed	Turbulence may trigger transition between pressure regimes	Coupled with obstacles and hydrogen concentration	[51,80]
External cloud formation	Formation and ignition of expelled unburned mixture	Can dominate maximum pressure through P_{ext}	Rapid turbulent external flame propagation	External explosion may block vent flow and amplify internal pressure	Coupled with vent area, ignition position and concentration	[19,60,74]

3.7. Coupled Parameter Effects and Transition of Dominant Pressure Peaks

As discussed in Section 2.2, the pressure history of a vented hydrogen explosion is commonly composed of several transient peaks associated with different physical mechanisms. The parameters presented in the previous subsections determine not only the magnitude of these peaks but also their relative importance. Consequently, the dominant pressure peak may shift from one mechanism to another as the combined conditions of the system change.

The available literature does not support a universal numerical threshold for these transitions. Reported changes in peak dominance are configuration-specific and should, therefore, be interpreted mechanistically rather than as fixed design limits. Nevertheless, several qualitative trends can be identified: remote ignition tends to favour stronger external explosions; congestion promotes flame acceleration and obstacle-induced internal peaks; restricted venting may lead to discharge-dominated pressure histories and low-resistance venting can reduce internal pressure but may increase the relevance of external cloud combustion if larger amounts of unburned mixture are expelled. Representative coupled conditions, their expected dominant pressure mechanisms and the corresponding engineering implications are summarised in Table 5.

Table 5. Representative coupled conditions and expected transition of dominant pressure mechanisms.

Coupled Condition	Expected Dominant Mechanism	Engineering Implication	References
Lean H_2-air mixture + elevated initial turbulence + large vent	External explosion peak may increase due to faster flame propagation, while flame-acoustic peaks may not scale proportionally	Do not assume that lean mixtures are always mild; validate both external explosion and acoustic/oscillatory peaks	[20]
Lean H_2-air mixture + back-wall ignition + high congestion or blockage	Obstacle-induced flame acceleration and flame-area peak; possible enhancement of external explosion if unburned mixture is expelled before flame arrival	Treat remote ignition and congestion as coupled worst-case drivers; blockage ratio alone is insufficient without obstacle position and flame path	[31,64,72]
Near-stoichiometric H_2-air mixture + front ignition + low activation pressure	Early vent opening and rapid flame arrival at the vent; weaker external cloud, but Helmholtz or flame-acoustic peaks may remain relevant	The limiting load may be an oscillatory or acoustically enhanced peak rather than a delayed external explosion peak	[14,33,49,53]
Near-stoichiometric H_2-air mixture + back-wall ignition + large vent area	Strong discharge of unburned mixture, larger external cloud and possible pressure feedback into the enclosure	External explosion and vent blockage should be assessed together with internal P_{red}; larger vents are not always equivalent to proportionally lower severity	[29,47,49]
High vent activation pressure or high vent inertia + reactive mixture	Stronger vent-opening peak and larger Helmholtz oscillation; acoustic peak may become dominant under some conditions	Vent-panel dynamics should be included in the design assessment, especially for low-strength enclosures and lightweight panels	[15,33,57]
Small vent area/high K_v + stoichiometric mixture	Restricted discharge; pressure response may shift towards a single broad internal maximum or residual internal combustion	Check whether the vent area is below the range where individual peaks remain distinguishable; avoid relying only on nominal vent area	[74]
Stratified mixture + upper rich layer + roof or raised vent	External explosion may dominate because the discharged cloud can be richer than the average enclosure composition	Use local maximum concentration and vent location, not only average hydrogen concentration, for design scenarios	[47,64]
Multiple vents or combined roof/side vents + non-homogeneous mixture	Multiple external-explosion peaks and altered internal pressure sequence	Evaluate peak sequence and spatial distribution of loads; total vent area alone may not describe the pressure response	[47]

For engineering design, the limiting dynamic load should, therefore, not be selected a priori from the name of the peak, such as vent-opening peak or external-explosion peak. The complete pressure-time history should be evaluated, and each relevant transient should be assessed in terms of pressure magnitude, duration, impulse and spatial distribution. In preliminary assessments, the governing load may often be identified as the highest internal overpressure, provided that this value includes all relevant pressure-generation mechanisms. However, in configurations involving lightweight structures, deformable panels, external confinement, or significant oscillatory pressure components, additional indicators such as impulse, pressure duration, reflected external loads and dynamic structural response may also be required.

4. Experimental and Numerical Investigations

Experimental research provides the principal basis for understanding vented hydrogen explosions, as it enables the identification of dominant physical mechanisms, the measurement of pressure and flame evolution, and the generation of validation data for numerical models and engineering correlations. In parallel, numerical modelling has become an essential complementary tool for investigating complex industrial configurations, exploring wide parametric ranges and assessing scenarios that are difficult, costly or unsafe to reproduce experimentally.

4.1. Experimental Investigations

The experimental literature covers a broad range of scales, from laboratory equipment to full-scale industrial installations. Figure 10 summarises this progression and illustrates the main trade-off between experimental control and industrial representativeness. Small-scale systems offer highly controlled and repeatable conditions, whereas larger facilities provide a more realistic representation.

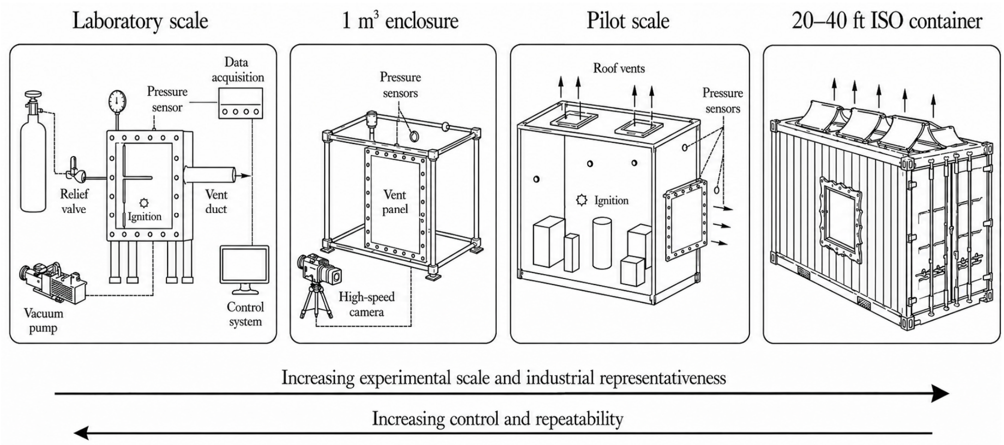

Figure 10. Overview of the main experimental scales used in vented hydrogen explosion research, from laboratory vessels to full-scale ISO containers.

Laboratory-scale tests are commonly used to characterise fundamental combustion parameters, deflagration indices, flame acceleration and transitions towards more severe combustion regimes [11,16,19,44]. Their main advantage lies in the precise control of initial conditions. However, their limited size restricts the reproduction of complex internal-external interactions and large-scale flow phenomena.

Facilities with volumes close to 1 m^3 provide an intermediate experimental scale and are widely used for parametric studies of concentration, ignition position, vent area, activation pressure and external explosion development [17,33,40,53]. These experiments offer a useful compromise between repeatability and physical relevance, allowing the identification of multiple pressure peaks, Helmholtz and flame-acoustic oscillations and transient interactions between the external explosion and the internal pressure field [33,74].

Pilot-scale chambers make it possible to investigate configurations that are more representative of industrial environments [47,64]. At this scale, studies can address stratified mixtures, multiple vent openings, non-uniform congestion, obstacle arrangements and scale-dependent pressure-generation mechanisms. Nevertheless, the increased complexity, cost and preparation time usually reduce the number of repeated tests and the range of parameters that can be examined.

Full-scale experiments in 20- and 40-foot ISO containers provide direct information on realistic industrial enclosures, including the influence of internal equipment, vent location, external explosion and structural deformation [26,55,80]. These tests are particularly valuable for evaluating actual load transmission and damage patterns, although their high cost and limited repeatability make systematic parametric analysis more difficult.

However, experimental data remain limited for near-real industrial hydrogen layouts. Actual installations, such as refuelling station cabinets, electrolyser rooms, compressor shelters or skid-mounted process units, often contain dense and irregular arrangements of vessels, valves, pipework, cable trays, control cabinets and auxiliary equipment. These elements may generate local turbulence, obstruct flame propagation, modify vent discharge paths and produce highly non-uniform pressure loads. Consequently, extrapolating results from empty or simplified congested enclosures to real industrial layouts remains subject to significant uncertainty.

A further limitation concerns instrumentation. Many experimental campaigns rely on a limited number of pressure sensors and optical access points, which may be sufficient to identify global trends but not to fully resolve the spatial distribution of pressure, flame arrival, external cloud combustion, or local loads on equipment. This limitation becomes more relevant as the enclosure geometry becomes larger and more complex, because local peaks or external pressure effects may not be captured by sparsely distributed measurements. Future large-scale experiments should, therefore, prioritise near-real equipment layouts together with denser pressure instrumentation, synchronised flame diagnostics and external pressure measurements, so that internal pressure histories, vent discharge, external explosion and local structural loads can be interpreted jointly.

From an instrumentation perspective, vented explosion experiments require high-speed and high-frequency measurement systems because the main pressure transients occur within a few milliseconds. Piezoelectric pressure transducers are commonly combined with high-speed cameras and optical techniques such as BOS-Schlieren to visualise the flame front, density gradients and the displacement of unburned mixture [16]. These methods are particularly useful for relating the timing of flame propagation and external cloud formation to the occurrence of individual pressure peaks.

The preparation of the hydrogen–air mixture is generally carried out using the partial-pressure method, followed by a homogenisation period before ignition [16]. Depending on the facility, ignition is produced using electrodes, spark systems, or equivalent controlled sources. The accuracy of mixture preparation, ignition positioning and synchronisation of pressure and optical measurements is essential for ensuring repeatability and for interpreting the origin of the recorded pressure transients.

Experimental campaigns consistently show that hydrogen concentration, vent area, ignition position, vent activation pressure, enclosure volume, geometry and congestion affect not only the maximum overpressure but also the timing and sequence of the pressure peaks [29,74]. In medium-scale enclosures, for example, the external explosion may temporarily oppose the vented flow and generate a secondary rise in internal pressure after the vent has opened [16]. Pressure-time histories also show that increasing hydrogen concentration can strongly intensify the first major pressure peak and the subsequent oscillatory response [29].

Overall, experimental investigations demonstrate that the severity of vented hydrogen explosions cannot be described by a single parameter. The observed response results from the combined influence of mixture reactivity, enclosure geometry, venting characteristics, ignition conditions, congestion and external surroundings. Table 6, therefore, summarises the main experimental campaigns reported in the literature, including enclosure volume, geometry and scale, venting configuration, mixture conditions, parameters investigated, principal limitations and main findings.

Table 6. Representative experimental studies on vented hydrogen explosions.

Volume and Geometry	Vent Configuration	Mixture Conditions	Parameters Investigated	Limitations	Main Findings	References
20 L sphere/cubic vessel	Vented and non-vented configurations, sometimes with ducts and bends	H_2-air mixtures, broad concentration range	H_2 concentration, P_{red}, dp/dt, P_{stat}, duct effects	Small scale; limited representation of industrial venting	Maximum pressure and pressure rise rate near 30% vol H_2; useful for deflagration indices	[11,44,68,70]
≈1 m^3 cubic/polyhedral vessel	Single vent, membranes or inertial panels	Homogeneous H_2-air mixtures, typically lean to near-stoichiometric	Concentration, ignition position, A_v, K_v, P_{burst}, external explosion	Scale still limited; sensitive to panel dynamics and initial turbulence	Multi-peak pressure behaviour; transition of dominant peak with concentration and K_v < = > 8.33	[74]
KIT ≈ 1 m^3 cubic enclosure	0.5 × 0.5 m frontal vent	Homogeneous H_2-air mixtures, including 18% vol	Rear ignition, pressure development, external flame	Empty enclosure; limited geometry variability	External explosion can block venting and generate the dominant internal pressure peak	[13,16]
1 m^3 rectangular enclosures	Top vent, 0.5 × 0.4 m	H_2-air mixtures from lean to rich	Concentration, pressure oscillations, external explosion	Specific top-vent geometry	P_{red} increased from low values at 19% H_2 to around 100 kPa at 39% H_2	[29,33,53]
27 m^3 chamber	Multiple vent areas and configurations	Homogeneous and/or stratified H_2-air mixture	Vent area, multi-vent effects, stratification	Limited number of large-scale repetitions	Larger vents reduce some internal peaks but may intensify external explosion contribution	[47,64]
63.7 m^3 chamber	Large vent area (5.4 m^2)	Homogeneous H_2-air mixtures, (12–15% vol)	External explosion, turbulence/acoustic effects, CFD validation	Usually limited number of concentration/configurations	First dominant peak often associated with external explosion; useful benchmark for CFD	[20,50]
ISO containers, 20–40 ft	Top, frontal or large-area venting	H_2-air mixtures in empty or congested containers	Scale, vent position, obstacles, structural response	High cost; limited repetitions; complex boundary conditions	Obstacles and structural dynamics modify pressure sequence and deformation response	[10,26,55,80]
Tubes and elongated ducts	Open, vented or ducted configurations	H_2-air mixtures across different concentrations	L/D, flame acceleration, DDT tendency, internal/external pressure	Not directly equivalent to industrial rooms or enclosures	L/D modifies balance between internal and external pressure; relevant for flame acceleration	[19,72]

4.2. Numerical Investigations

Numerical modelling has progressively evolved from simplified empirical correlations and prescriptive engineering methods towards computational fluid dynamics (CFD) tools capable of representing combustion, turbulence, vent discharge, obstacle interaction and pressure-wave propagation [12,18,82,83]. This development responds to the inherent limitations of experimental campaigns, which cannot systematically reproduce the wide range of geometries, mixture conditions, venting configurations and external environments encountered in industrial applications.

Empirical correlations and simplified design models remain useful for preliminary assessments because they provide rapid estimates of reduced explosion pressure and venting requirements. However, these approaches generally represent the event through a limited number of global parameters and cannot adequately distinguish the mechanisms responsible for the different pressure peaks [35,84]. In vented hydrogen explosions, this limitation is particularly relevant because the maximum pressure may originate from external cloud combustion, residual internal burning, acoustic oscillations, restricted discharge, or flame interaction with obstacles.

Among the CFD tools used in hydrogen safety studies, FLACS® is one of the most widely applied in industrial risk assessment. The code uses a Reynolds-Averaged Navier-Stokes formulation and represents complex geometries through distributed porosity and sub-grid models for turbulence generation and flame acceleration [12]. Its combustion framework includes hydrogen-specific treatments for burning velocity, flammability limits and preferential-diffusion effects in lean mixtures [48,58,77]. Nevertheless, the accuracy of the predictions remains strongly dependent on mesh resolution, boundary conditions, obstacle representation, vent-panel modelling and the internal parameters of the combustion model [76,82,85].

Other CFD codes, including ANSYS Fluent®, ANSYS CFX®, ADREA-HF® and OpenFOAM®, have also been applied to vented hydrogen explosions [18,30,83,86]. These tools provide greater flexibility in the selection of turbulence, combustion and boundary-condition models, making them suitable for the detailed analysis of specific configurations. Large Eddy Simulation approaches are particularly valuable when large turbulent structures, flame wrinkling, or obstacle-induced recirculation must be resolved more explicitly [10,11,39,50]. However, their computational cost continues to limit their systematic application to large industrial domains and extensive parametric studies.

Direct comparisons between CFD predictions and experiments are essential for assessing the strengths and limitations of each model. Figure 11 compares experimental data with predictions from FLACS®, FLUENT®, CFX® and ADREA-HF® for a vented hydrogen explosion in a 64 m^3 chamber [87]. Three indicators are considered: maximum overpressure, time to maximum overpressure and flame speed at a propagation distance of 4 m.

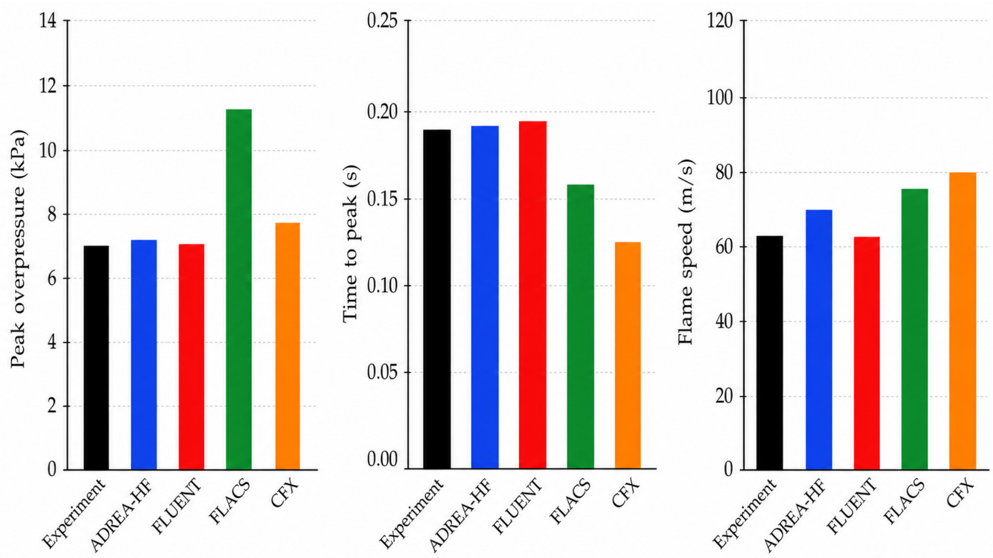

Figure 11. Comparison of experimental results and CFD predictions for a vented hydrogen explosion in a 64 m^3 chamber. Adapted from [87].

FLUENT® and ADREA-HF® reproduce the measured maximum overpressure particularly well, with predictions of 7.10 and 7.15 kPa, respectively, compared with the experimental value of 7.0 kPa. CFX® provides a slightly higher estimate of 7.69 kPa, whereas FLACS® overpredicts the peak, reaching approximately 11.3 kPa. For the time to peak pressure, ADREA-HF® and FLUENT® remain relatively close to the experimental value of 0.19 s, while FLACS® and CFX® predict an earlier maximum. At a distance of 4 m from the ignition point, the experimental flame speed is approximately 62 m/s. FLUENT® provides the closest value, whereas ADREA-HF®, FLACS® and CFX® progressively overestimate the flame-propagation velocity.

These results show that model performance depends on the output variable considered. A code may reproduce the maximum overpressure while showing larger deviations in peak timing, flame speed, or external pressure development. This is particularly relevant for vented explosions because conservative prediction of internal overpressure does not necessarily imply conservative prediction of the complete venting sequence. If the flame speed is artificially accelerated, the predicted time between vent opening and flame arrival at the vent may be shortened, modifying the amount of unburned mixture discharged before ignition of the external cloud and potentially altering the predicted severity of the secondary external explosion.

For this reason, CFD validation should not be based solely on a single global parameter. For regulatory or engineering qualification, the applicability range of the model should first be defined, and simulations should then be compared with representative experiments using multiple indicators, including maximum internal overpressure, time to peak pressure, pressure-rise rate or impulse, flame arrival time or flame speed, external pressure field and secondary or oscillatory pressure peaks [80,87–89]. The validation process should also include mesh-sensitivity analysis and checks of the vent-panel model, obstacle representation and boundary conditions, with acceptable performance demonstrated across more than one validation case.

Overall, CFD tools can reproduce the main pressure rise and the general flame-propagation trend with reasonable accuracy when the selected models and boundary conditions are appropriately validated. However, greater uncertainty remains in the prediction of secondary pressure peaks, high-frequency oscillations, flame-acoustic coupling and transient interactions between internal combustion and external venting [87]. Some models may also provide conservative estimates in large-scale or strongly coupled configurations [90]. Consequently, the credibility of a numerical analysis depends not only on the selected software, but also on the turbulence and combustion models, mesh sensitivity, vent representation, boundary conditions and validation against experiments representative of the intended application.

Surrogate and Data-Driven Models for Rapid Screening

Building on the limitations identified above, surrogate and data-driven models have emerged as complementary tools to extend the practical use of numerical modelling. While CFD remains necessary for detailed consequence assessment, its computational cost makes exhaustive exploration of the design and accident scenario space difficult. Surrogate models are, therefore, intended to support preliminary screening, sensitivity analysis and the selection of critical scenarios for subsequent high-fidelity assessment, rather than to replace validated CFD or experiments.

Artificial neural networks and multilayer perceptron models have been applied to vented gas explosion databases to estimate reduced overpressure from variables such as gas type, concentration, enclosure geometry, vent area, activation pressure and ignition location [91]. Similar approaches have been trained on CFD-generated hydrogen–air explosion datasets to predict peak overpressure, pressure-rise rate and impulse at very low computational cost [59]. Theory-guided machine-learning models can improve interpretability by combining explosion mechanics with data-driven regression [92].

Other surrogate strategies may also be useful for explosion relief design. Gaussian-process emulators and response-surface models are attractive for small datasets because they can provide uncertainty estimates together with the prediction, while reduced-order models can approximate families of simulations at lower cost. Physics-informed neural networks may improve physical consistency by incorporating conservation laws, boundary conditions, or residual constraints, although their application to turbulent, compressible and multi-peak vented hydrogen explosions remains at an early stage.

Graph neural networks are particularly promising for complex industrial layouts because they can operate on mesh- or graph-based representations of irregular geometries. Recent GNN-based approaches have predicted pressure, temperature and velocity fields for hydrogen–air deflagrations in complex, congested and confined environments from URANS-generated data, with computational speed-ups of up to three orders of magnitude compared with CFD [93].

Despite these advantages, surrogate models remain strongly dependent on the quality, physical fidelity and coverage of the training data. If trained from CFD, they may reproduce the biases of the underlying turbulence, combustion, venting, or geometry model; if trained from experiments, the database is usually sparse and configuration-specific. Therefore, extrapolation to different scales, vent-panel behaviours, congestion patterns, stratified mixtures, or external confinement conditions should be avoided unless additional validation is performed.

For engineering use, surrogate models should be considered rapid screening tools rather than stand-alone vent-sizing methods. Their validation should, therefore, be consistent with the multi-index framework described above for CFD models, while also accounting for the quality, coverage and physical fidelity of the training database.

Finally, Table 7 summarises the main numerical approaches used in the literature for vented hydrogen explosions, including the turbulence and combustion formulations adopted, the validation configurations considered, the volume, geometry, vent configuration and phenomena analysed and the principal limitations and findings reported.

Table 7. Representative numerical studies on vented hydrogen explosions.

CFD/Model Approach	Turbulence/ Combustion Model	Validation	Volume and Geometry	Vent Configuration	Analysed Phenomena	Limitations	Main Findings	Refs
Empirical/ normative correlations	Semi-empirical vent sizing based on P_{red}	Comparison with experimental databases	Simplified vessels and standard geometries	Standard vent assumptions	P_{red} estimation, vent area sizing	Single-peak approach; limited for obstacles, stratification and H_2-rich mixtures	Useful for preliminary design but limited for full H_2 phenomenology	[35,84,94]
Phenomenological models	Mechanistic decomposition of pressure peaks	Comparison with selected vented explosion tests	Generic vented enclosures	Direct venting	External explosion, flame-acoustic coupling, obstacle-induced flame area	Requires empirical data for flame area and turbulent burning velocity	Helps explain why dominant peak changes with configuration	[42,50,95]
FLACS® (FLACS-Hydrogen)	k-ε; flame acceleration (β-flame) and porosity models	Small-, medium- and large-scale experiments; benchmarks	Vented enclosures, containers, congested volumes	Direct vents, top/frontal vents, industrial layouts	Pressure development, flame acceleration, congestion, external loads	Sensitive to mesh, boundary conditions and panel modelling; limited transient instability resolution	Robust engineering tool; often conservative in complex or congested scenarios	[12,48,58,76,88]
ANSYS Fluent®/CFX®	Fluent: LES; Multi-phen. burning velocity CFX: k-ε; Zimont model	Laboratory and selected vented experiments	Small and medium enclosures, ducts	Direct venting and ducted venting	Internal/external combustion, jet structure, pressure propagation	High dependence on combustion model and boundary conditions	Useful for detailed analysis of flow and external flame structure	[18,30,67,82,83, 86]

Table 7. *Cont.*

CFD/Model Approach	Turbulence/ Combustion Model	Validation	Volume and Geometry	Vent Configuration	Analysed Phenomena	Limitations	Main Findings	Refs
OpenFOAM®/ HyFOAM®	LES; k-eq. eddy viscosity model	Small-scale and obstacle experiments	Tubes, obstructed chambers, lean H_2 mixtures	Confined or vented configurations	Flame wrinkling, instability growth, lean H_2 combustion	High computational cost; limited industrial-scale validation	Better representation of turbulence-flame interaction and instabilities	[10,11,39]
ADREA-HF®	LES; Multi-phen. burning velocity	Experimental validation and benchmark cases	Enclosures and hydrogen safety scenarios	Confined or vented configurations	Pressure development, dispersion and combustion coupling	Less widely benchmarked than FLACS®/ANSYS® for vented explosions	Useful complementary tool for hydrogen risk assessment	[16,37,87,96]
Benchmark/blind prediction studies	Multiple CFD tools and users	Large-scale experiments and container tests	Different chambers, containers and complex layouts	Large vents, industrial venting arrangements	Code-to-code variability, external pressure, structural response	Significant user dependence and mesh/model sensitivity	CFD can be reliable for engineering use, but uncertainty remains high for external fields	[10,76,81,87]

Overall, experimental and numerical research has substantially improved the understanding of vented hydrogen explosions, particularly regarding external combustion, multi-peak pressure development, concentration effects and congestion-induced flame acceleration. Nevertheless, important uncertainties remain in scale extrapolation, prediction of external loads, structural response, realistic vent-panel behaviour and validation in complex industrial geometries. Addressing these limitations requires an integrated approach combining well-instrumented experiments, phenomenological interpretation and rigorously validated CFD simulations. Such a framework is essential for translating current scientific knowledge into reliable engineering methods and design criteria for hydrogen installations.

5. Codes, Standards and Design Approaches

The design of explosion-venting systems is primarily based on engineering standards and calculation methods derived from experimental data and empirical correlations for flammable gases in general. Although these approaches have subsequently been applied to hydrogen, the increasing deployment of hydrogen production, storage and utilisation technologies has revealed various limitations in conventional design methods. Among the most widely used references are the European standard EN 14994:2007 [97] and the American standard NFPA 68:2023 [98], both of which focus on the sizing of venting areas and the estimation of the maximum reduced overpressure (P_{red}) [80].

Early vent-sizing methods were largely developed from experiments involving hydrocarbon-air mixtures and relatively simple enclosure geometries [35]. Their principal advantage is that they reduce a complex transient phenomenon to a manageable set of design parameters and a single reduced pressure value. This facilitates preliminary engineering calculations and regulatory consistency, but provides limited information on the mechanisms responsible for the pressure response.

In Europe, EN 14994 is currently the most widely used standard for the design of venting systems for gas explosions. The standard establishes calculation procedures based on parameters such as the gas explosion constant (K_G), the volume of the enclosure, the panel activation pressure (P_{stat}) and the permissible reduced overpressure [97]. However, its scope of applicability is relatively limited for hydrogen mixtures, as it is only valid for $K_G \leq 550$ bar·m/s, in isolated compact enclosures, corresponding approximately to concentrations below 20–25% vol of H_2, and assumes empty enclosures or low congestion [80,95]. The standard itself acknowledges that the presence of obstacles or elements generating turbulence can significantly increase the severity of the explosion and require advanced methodologies or specific experimental validations.

Meanwhile, NFPA 68 incorporates formulations that are partially closer to the actual physics of deflagration, using parameters related to laminar combustion velocity and certain effects associated with turbulence [88,98]. Furthermore, it explicitly accounts for certain internal congestion factors and can be applied to larger enclosures and higher geometric ratios than those considered in EN 14994. Comparative studies generally indicate that its predictions may be conservative for some hydrogen configurations, although the degree of conservatism varies with enclosure geometry, ignition location and venting conditions [87,88]. Consequently, neither EN 14994 nor NFPA 68 should be regarded as universally conservative or uniformly accurate for all hydrogen applications.

Figure 12 compares the performance of EN 14994, NFPA 68 and two empirical models developed by FM Global and Molkov for different ignition locations [94]. The results are expressed as the ratio between modelled and measured maximum overpressure. A value of unity represents exact agreement; values above unity indicate overprediction and values below unity indicate underprediction.

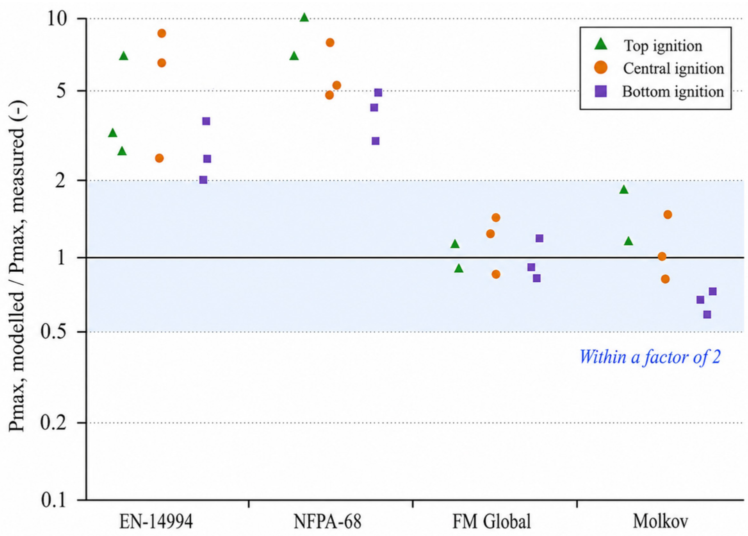

Figure 12. Ratio between modelled and measured maximum overpressure for EN 14994, NFPA 68, FM Global and Molkov models under different ignition locations. Adapted from [94].

As can be seen, EN 14994 and NFPA 68 predominantly overpredict the measured maximum overpressure, with several estimates substantially exceeding the upper factor-of-two limit. This tendency is particularly evident for top and central ignition in the analysed configurations. By contrast, the FM Global model produces predictions clustered more closely around unity, with all selected values remaining within a factor of two. The Molkov model also provides comparatively close agreement, although most predictions lie below unity and, therefore, indicate a general tendency towards underprediction. This is relevant from a safety perspective because proximity to unity should not be interpreted as sufficient for safety-critical design when part of the validation range is underpredicted. Any safety margin or correction factor for advanced empirical models should, therefore, be defined from the bias, scatter and lower-bound performance of the model against representative validation data, rather than adopted as a universal factor. In the absence of a configuration-specific correction or independent validation, such models should be used only as comparative tools or preliminary estimates. The results further show that the predictive error depends on ignition position, confirming that model performance cannot be assessed independently of the flame-propagation path and vent location.

The comparison demonstrates that the suitability of an engineering model cannot be judged solely by whether it is nominally conservative. Excessive overprediction may lead to unnecessarily large vents and practical design constraints, whereas underprediction may result in insufficient pressure relief or inadequate structural resistance. Therefore, moving from standard correlations to validated CFD should not be understood as a rejection of standards, but as a transition from preliminary normative sizing to case-specific consequence assessment. This transition is justified when the configuration lies outside the applicability range of the standard, when the predicted vent area or reduced pressure is highly sensitive to small changes in input parameters, or when relevant mechanisms are not explicitly represented by the correlation. Typical triggering conditions include high or irregular congestion, non-standard geometries, multiple or ducted vents, significant vent-panel inertia, stratified mixtures, external confinement near the vent outlet and strong internal-external coupling. In such cases, standard calculations should be retained as a reference baseline, while the final design should be supported by validated CFD, sensitivity analysis and, where necessary, dedicated testing.

Explosion-venting design must also be integrated into the wider regulatory framework for explosive atmospheres. In the European Union, Directive 1999/92/EC establishes minimum requirements for protecting workers potentially exposed to explosive atmospheres, while Directive 2014/34/EU addresses equipment and protective systems intended for use in such environments [99,100]. Complementary standards include EN 14797 for explosion venting devices, EN 14460 for explosion-resistant equipment and EN 1127-1 for general principles of explosion prevention and protection [101–103]. Hydrogen-specific guidance, including NFPA 2 and ISO/TS 15916, provides additional recommendations concerning the characteristic hazards and safe use of hydrogen systems [104,105].

Current codes and standards remain essential for preliminary design, compliance assessment and the specification of protective systems. Nevertheless, empirical correlations have inherent limitations when applied to highly reactive hydrogen mixtures, congested layouts, non-standard geometries, or configurations involving strong internal-external coupling. In such cases, standard calculations should be supplemented by experimentally validated CFD simulations, sensitivity analyses and, where necessary, dedicated testing [35,84]. Table 8 summarises the principal codes, standards and engineering approaches currently applied to the assessment and design of venting systems for hydrogen explosions.

Table 8. Codes, standards and engineering approaches in the design of venting systems.

Document (Name)	Type of Document	Design Basis	Limitations	Applications	References
EN 14994:2007	Standard. Gas explosion venting protective systems	Empirical correlations based on K_G, V, P_{red} and P_{stat}	Applicable up to $K_G \leq 550$ bar·m/s in isolated compact enclosures; low congestion and turbulence effect	Empty vessels, compact enclosures, preliminary vent sizing	[97]
NFPA 68:2023	Standard. Explosion protection by deflagration venting	Correlations based on laminar burning velocity and turbulence effects	Conservative predictions; limited treatment of highly complex geometries	Industrial vent sizing, partially congested enclosures	[98]
ISO/TS 15916:2026	Technical Specification. Hydrogen technologies. Basic considerations for safety	General hydrogen safety principles and risk mitigation	Non-prescriptive engineering framework	Hydrogen systems and installations	[105]
NFPA 2:2026	Standard. Hydrogen technologies code	Hydrogen-specific safety requirements	General guidance, not detailed vent design methodology	Hydrogen facilities and infrastructures	[104]

https://doi.org/10.3390/app16147046

Table 8. *Cont.*

Document (Name)	Type of Document	Design Basis	Limitations	Applications	References
EN 14797:2006	Standard. Explosion venting devices	Design and testing requirements for vent devices	Its application in pipelines or uses not covered by EN 14994 requires specific technical validation and, where appropriate, additional testing	Vent panels and explosion vent devices	[101]
EN 14460:2018	Standard. Explosion-resistant equipment	Structural resistance against explosion pressure	Complementary to venting systems	Explosion-resistant vessels and equipment	[102]
ATEX Directives (1999/92/CE, 2014/34/UE)	European regulatory framework	Prevention, ignition control and mitigation of explosive atmospheres	Not specific to vent sizing	Industrial safety, hazardous areas and equipment requirements	[99,100]

6. Conclusions and Future Directions

Vented hydrogen explosions are governed by strongly coupled combustion, fluid-dynamic, geometric, structural and external phenomena. The literature reviewed demonstrates that their severity cannot be characterised solely by the maximum reduced overpressure, since the pressure response commonly comprises several transient peaks associated with vent opening, external cloud combustion, residual internal burning, Helmholtz oscillations, flame-acoustic coupling and obstacle-induced flame acceleration.

Hydrogen concentration, ignition position, vent area and activation pressure, enclosure geometry, scale and internal or external congestion influence not only the magnitude of the pressure load, but also its timing, dominant origin and spatial distribution. Their effects are highly interdependent, meaning that trends observed for an isolated parameter cannot always be generalised to different configurations. In particular, external explosion, congestion, stratification and vent-outlet surroundings may reduce the effective performance of the venting system and generate pressure loads that are not adequately represented by simplified single-peak descriptions.

Experimental campaigns conducted from laboratory to full scale have substantially improved the phenomenological understanding of vented hydrogen explosions and provided essential data for model validation. Nevertheless, important uncertainties remain regarding scale extrapolation, mixture stratification, realistic vent-panel dynamics, local congestion effects, external confinement, instrumentation density and structural response. The diversity of test geometries, boundary conditions and measurement strategies also complicates direct comparison between experimental datasets.

CFD tools can reproduce the principal pressure and flame-propagation trends when appropriately configured and validated. However, their performance remains dependent on the combustion and turbulence formulations, mesh resolution, boundary conditions, representation of congestion, vent-panel dynamics and the experimental database used for validation. Agreement in maximum overpressure alone is, therefore, insufficient to demonstrate predictive capability; validation should also consider peak timing, pressure-rise rate, impulse, flame speed or arrival time, secondary transients and external pressure fields. Surrogate and data-driven models may support rapid screening and sensitivity analysis, but their use for engineering purposes requires the same multi-index validation logic and careful consideration of the quality and applicability of the training data.

Engineering standards such as EN 14994:2007 and NFPA 68:2023 remain essential for preliminary vent sizing and safety assessment. However, their empirical basis and simplified assumptions limit their direct applicability to highly reactive mixtures, congested enclosures, non-standard geometries, stratified atmospheres, and configurations involving strong internal-external coupling. Their use in such scenarios should, therefore, be complemented by sensitivity analyses, validated numerical simulations and, where justified, dedicated experimental testing.

Future research should prioritise well-instrumented large-scale campaigns representative of industrial hydrogen installations, including realistic equipment layouts, stratified mixtures, multiple vents, ducted venting, external confinement and deformable vent panels. Greater attention should also be given to the coupled prediction of internal pressure, external flame and pressure loads, pressure-time histories, impulse and structural response. Future vent-sizing approaches should move towards coupled explosion-structure assessment, combining pressure-time histories, external reflected loads and non-linear structural dynamics to evaluate ultimate limit states such as plastic deformation, local buckling or loss of structural integrity, rather than relying only on maximum internal pressure.

Finally, coordinated benchmark exercises, standardised reporting procedures and shared experimental databases are required to improve model validation and reduce uncertainty. Integrating experimental evidence, phenomenological interpretation, CFD modelling, structural assessment and engineering standards will be essential for developing more reliable and broadly applicable explosion-venting design methods for future hydrogen infrastructure.

Author Contributions: Conceptualization, Á.R.-G. and D.B.; methodology, J.P.C., Á.R.-G. and D.B.; software, J.P.C.; formal analysis, J.P.C.; investigation, J.P.C., Á.R.-G. and D.B.; resources, D.B., Á.R.-G. and N.V.; data curation, J.P.C.; writing—original draft preparation, J.P.C., Á.R.-G. and D.B.; writing—review and editing, J.P.C., Á.R.-G., I.A., B.C., D.L., V.V., N.V. and D.B.; visualization, J.P.C.; supervision, Á.R.-G. and D.B. All authors have read and agreed to the published version of the manuscript.

Funding: This research received no external funding.

Institutional Review Board Statement: Not applicable.

Informed Consent Statement: Not applicable.

Data Availability Statement: No new data were created or analyzed in this study. Data sharing is not applicable to this article.

Acknowledgments: The authors are grateful to Spanish "Ministerio de Ciencia, Innovación y Universidades" for the FPU24/00522 grant.

Conflicts of Interest: The authors declare no conflicts of interest.

Abbreviations

The following abbreviations are used in this manuscript:

EU	European Union
HIAD	Hydrogen Incidents and Accidents Database
JRC	European Commission's Joint Research Centre
CFD	Computational Fluid Dynamics
DDT	Deflagration-to-Detonation Transition
BOS	Background Oriented Schlieren Method

References

1. Ishaq, H.; Dincer, I.; Crawford, C. A review on hydrogen production and utilization: Challenges and opportunities. *Int. J. Hydrogen Energy* **2022**, *47*, 26238–26264. [CrossRef]
2. European Commission. European Green Deal. 2019. Available online: https://commission.europa.eu/strategy-and-policy/priorities-2019-2024/european-green-deal_es (accessed on 27 May 2026).
3. United Nations. Paris Agreement. 2015. Available online: https://unfccc.int/process-and-meetings/the-paris-agreement (accessed on 27 May 2026).

4. Qureshi, F.; Yusuf, M.; Kamyab, H.; Zaidi, S.; Junaid Khalil, M.; Arham Khan, M.; Azad Alam, M.; Masood, F.; Bazli, L.; Chelliapan, S.; et al. Current trends in hydrogen production, storage and applications in India: A review. *Sustain. Energy Technol. Assess.* **2022**, *53*, 102677. [CrossRef]
5. European Commission. A Hydrogen Strategy for a Climate-Neutral Europe. 2020. Available online: https://energy.ec.europa.eu/system/files/2020-07/hydrogen_strategy_0.pdf (accessed on 27 May 2026).
6. Gobierno de España. Hoja de ruta del Hidrógeno: Una Apuesta por el Hidrógeno Renovable. 2020. Available online: https://www.miteco.gob.es/content/dam/miteco/es/ministerio/planes-estrategias/hidrogeno/hojarutahidrogenorenovable_tcm30-525000.PDF (accessed on 27 May 2026).
7. Rivard, E.; Trudeau, M.; Zaghib, K. Hydrogen storage for mobility: A review. *Materials* **2019**, *12*, 1973. [CrossRef] [PubMed]
8. Bessarabov, D. PEM water electrolysis. In *Hydrogen and Fuel Cells Primers*; Elsevier: Amsterdam, The Netherlands, 2018.
9. European Commission. *European Hydrogen Incidents and Accidents Database HIAD 2.2*; Joint Research Centre: Petten, The Netherlands, 2026. Available online: https://minerva.jrc.ec.europa.eu/en/shorturl/capri/hiadpt (accessed on 27 May 2026).
10. Skjold, T.; Hisken, H.; Bernard, L.; Mauri, L.; Atanga, G.; Lakshmipathy, S.; Lucas, M.; Carcassi, M.; Schiavetti, M.; Chandra Madhav Rao, V.; et al. Blind-prediction: Estimating the consequences of vented hydrogen deflagrations for inhomogeneous mixtures in 20-foot ISO containers. *J. Loss Prev. Process Ind.* **2019**, *61*, 220–236. [CrossRef]
11. Li, R.; Malalasekera, W.; Ibrahim, S. Numerical study of vented hydrogen explosions in a small scale obstructed chamber. *Int. J. Hydrogen Energy* **2018**, *43*, 16667–16683. [CrossRef]
12. Lakshmipathy, S.; Skjold, T.; Hisken, H.; Atanga, G. Consequence models for vented hydrogen deflagrations: CFD vs. engineering models. *Int. J. Hydrogen Energy* **2019**, *44*, 8699–8710. [CrossRef]
13. Kuznetsov, M.; Friedrich, A.; Stern, G.; Kotchourko, N.; Jallais, S.; L'Hostis, B. Medium-scale experiments on vented hydrogen deflagration. *J. Loss Prev. Process Ind.* **2015**, *36*, 416–428. [CrossRef]
14. Cao, Y.; Sun, A.; Hua, M.; Pan, X. Dynamic and flame evolution vented hydrogen-air mixtures explosion with effect of concentration and ignition location. *Int. J. Hydrogen Energy* **2025**, *161*, 150701. [CrossRef]
15. Chu, Z.; Chen, R.; Li, X.; Xu, Z.; Shi, X.; Cao, W.; Fu, G.; Xu, J.; Zhou, W.; Zhang, Y. Characteristics of hydrogen/air premixed explosion venting in a cabinet vessel under different bursting pressures. *Int. J. Hydrogen Energy* **2025**, *186*, 151981. [CrossRef]
16. Tolias, I.C.; Venetsanos, A.G.; Kuznetsov, M.; Koutsoukos, S. Evaluation of an improved CFD model against nine vented deflagration experiments. *Int. J. Hydrogen Energy* **2021**, *46*, 12407–12419. [CrossRef]
17. Li, H.; Tang, Z.; Li, J.; Guo, J.; Zhang, J.; Li, Q. Investigation of vented hydrogen-air deflagrations in a congested vessel. *Process Saf. Environ. Prot.* **2019**, *129*, 196–201. [CrossRef]
18. Li, J.; Hao, H. Internal and external pressure prediction of vented gas explosion in large rooms by using analytical and CFD methods. *J. Loss Prev. Process Ind.* **2017**, *49*, 367–381. [CrossRef]
19. Cao, Y.; Wang, Y.; Song, X.; Xing, H.; Li, B.; Xie, L. External overpressure of vented hydrogen-air explosion in the tube. *Int. J. Hydrogen Energy* **2019**, *44*, 32343–32350. [CrossRef]
20. Bauwens, C.R.; Dorofeev, S.B. Effect of initial turbulence on vented explosion overpressures from lean hydrogen-air deflagrations. *Int. J. Hydrogen Energy* **2014**, *39*, 20509–20515. [CrossRef]
21. Fakandu, B.M.; Andrews, G.E.; Phylaktou, H.N. Vent burst pressure effects on vented gas explosion reduced pressure. *J. Loss Prev. Process Ind.* **2014**, *36*, 429–438.
22. Bjerketvedt, D.; Bakke, J.R.; van Wingerden, K. *Gas Explosion Handbook*; GEXCON: Bergen, Norway, 2022.
23. Vyazmina, E.; Jallais, S. Validation and recommendations for FLACS CFD and engineering approaches to model hydrogen vented explosions: Effects of concentration, obstruction vent area and ignition position. *Int. J. Hydrogen Energy* **2016**, *41*, 15101–15109. [CrossRef]
24. Bauwens, C.R.; Chaffee, J.; Dorofeev, S.B. Vented explosion overpressures from combustion of hydrogen and hydrocarbon mixtures. *Int. J. Hydrogen Energy* **2011**, *36*, 2329–2336. [CrossRef]
25. Molkov, V.; Dobashi, R.; Suzuki, M.; Hirano, T. Modeling of vented hydrogen-air deflagrations and correlations for vent sizing. *J. Loss Prev. Process Ind.* **1999**, *12*, 147–156. [CrossRef]
26. Hao, T.T.; Wang, C.J.; Yan, W.J.; Ren, W.X.; Yuen, K.V. Experimental investigation on the dynamic responses of vented hydrogen explosion in a 40-foot container. *Int. J. Hydrogen Energy* **2021**, *46*, 19229–19243. [CrossRef]
27. García Torrent, J. *Seguridad Industrial en Atmósferas Explosivas*; Laboratorio Oficial Madariaga: Madrid, Spain, 2003.
28. Bauwens, C.R.; Chao, J.; Dorofeev, S.B. Effect of hydrogen concentration on vented explosion overpressures from lean hydrogen-air deflagrations. *Int. J. Hydrogen Energy* **2012**, *37*, 17599–17605. [CrossRef]
29. Wang, J.; Guo, J.; Yang, F.; Zhang, J.; Lu, S. Effects of hydrogen concentration on the vented deflagration of hydrogen-air mixtures in a 1-m^3 vessel. *Int. J. Hydrogen Energy* **2018**, *43*, 21161–21168. [CrossRef]
30. Zhao, H.; Meng, X.; Zhu, W.; Xu, J.; Bi, M. Effects of initial temperature and pressure on hydrogen explosion venting characteristics: A numerical simulation study. *Int. J. Hydrogen Energy* **2025**, *155*, 150360. [CrossRef]

31. Tomlin, G.; Johnson, D.M.; Cronin, P.; Phylaktou, H.N.; Andrews, G.E. The effect of vent size and congestion in large-scale vented natural gas/air explosions. *J. Loss Prev. Process Ind.* **2015**, *35*, 169–181. [CrossRef]
32. Wang, F.; Huang, S.; Xu, C.; Wang, C.; Guo, J.; Lin, J. Experimental and numerical study on vented H_2/air explosion in an obstructed duct: Effects of hydrogen concentration and vent size. *Int. J. Hydrogen Energy* **2025**, *143*, 330–339. [CrossRef]
33. Rui, S.; Guo, J.; Li, G.; Wang, C. The effect of vent burst pressure on a vented hydrogen–air deflagration in a 1 m^3 vessel. *Int. J. Hydrogen Energy* **2018**, *43*, 21169–21176. [CrossRef]
34. Huang, S.; Guo, J.; Mei, L.; Wang, F.; Wang, C.; Lin, J. Experiments on vented H_2/CH_4/air explosion in a chamber with a hinged panel: Effects of hydrogen volume fraction. *J. Loss Prev. Process Ind.* **2025**, *94*, 105546. [CrossRef]
35. Mohd Mokhtar, K.; Md Kasmani, R.; Che Hassan, C.R.; Hamid, M.D.; Davazdah Emami, S.; Mohamad Nor, M.I. Reliability and applicability of empirical equations in predicting the reduced explosion pressure of vented gas explosions. *J. Loss Prev. Process Ind.* **2020**, *63*, 104023. [CrossRef]
36. Li, Y.; Bi, M.; Zhou, Y.; Zhang, Z.; Zhang, K.; Gao, W. Evaluation of unrestricted hydrogen and hydrogen-methane explosion venting through duct. *Int. J. Hydrogen Energy* **2021**, *46*, 7011–7021. [CrossRef]
37. Tolias, I.C.; Venetsanos, A.G.; Markatos, N.C.; Kiranoudis, C.T. CFD simulation of hydrogen deflagration in a vented room. *J. Phys. Conf. Ser.* **2015**, *640*, 012036. [CrossRef]
38. Yang, K.; Wang, R.; Shen, J.; Lv, P. Characteristics of external overpressure and flame evolution induced by hydrogen explosion venting. *Int. Commun. Heat Mass Transf.* **2026**, *175*, 111039. [CrossRef]
39. Sheng, Z.; Yang, G.; Gao, W.; Li, S.; Shen, Q.; Sun, H. Study on the dynamic process of premixed hydrogen-air deflagration flame propagating in a closed space with obstacles. *Fuel* **2023**, *334*, 126542. [CrossRef]
40. Schiavetti, M.; Pini, T.; Carcassi, M. The effect of venting process on the progress of a vented deflagration. *Int. J. Hydrogen Energy* **2019**, *44*, 9080–9088. [CrossRef]
41. Schiavetti, M.; Carcassi, M. Analysis of acoustic pressure oscillation during vented deflagration and proposed model for the interaction with the flame front. *Int. J. Hydrogen Energy* **2017**, *42*, 7707–7715. [CrossRef]
42. Chao, J.; Bauwens, C.R.; Dorofeev, S.B. An analysis of peak overpressures in vented gaseous explosions. *Proc. Combust. Inst.* **2011**, *33*, 2367–2374. [CrossRef]
43. Atanga, G.; Lakshmipathy, S.; Skjold, T.; Hisken, H.; Hanssen, A.G. Structural response for vented hydrogen deflagrations: Coupling CFD and FE tools. *Int. J. Hydrogen Energy* **2019**, *44*, 8893–8903. [CrossRef]
44. Zhang, X.; Ma, T.; Xu, Z.; Li, X.; Cao, W.; Shi, X.; Jiao, F.; Yu, C.; Shu, C.M.; Zhang, Y. Flame dynamics and pressure response of hydrogen explosion within closed and venting environments. *Process Saf. Environ. Prot.* **2025**, *204*, 108079. [CrossRef]
45. Yao, Y.; Pan, A.; Tan, L.; Hu, M.; Wang, Y. Optimization of design parameters of hydrogen storage compartment sidewall vents for hydrogen fuel cell buses. *Fuel* **2026**, *404*, 136327. [CrossRef]
46. Duan, Z.; Guo, J.; Wang, X.; Li, J.; Zhang, S.; Yang, F. Experiments on vented deflagration of stoichiometric hydrogen–methane–air mixtures: Effect of hydrogen fraction. *Int. J. Hydrogen Energy* **2020**, *45*, 25615–25622. [CrossRef]
47. Chen, Y.; Li, Y.; Li, Z.; Ji, C.; Liu, X. Effect of vent area, vent location and number of vents on vented hydrogen deflagrations in a 27 m^3 chamber. *Int. J. Hydrogen Energy* **2020**, *45*, 31268–31277. [CrossRef]
48. Chen, Y.; Yuan, D.; Guo, J.; Liu, X. Research on mechanism and influence factors of the overpressure development in vented hydrogen deflagrations based on numerical simulation. *Int. J. Hydrogen Energy* **2019**, *44*, 22681–22690. [CrossRef]
49. Guo, J.; Sun, X.; Rui, S.; Cao, Y.; Hu, K.; Wang, C. Effect of ignition position on vented hydrogen–air explosions. *Int. J. Hydrogen Energy* **2015**, *40*, 15780–15788. [CrossRef]
50. Keenan, J.J.; Makarov, D.V.; Molkov, V.V. Rayleigh-Taylor instability: Modelling and effect on coherent deflagrations. *Int. J. Hydrogen Energy* **2014**, *39*, 20467–20473. [CrossRef]
51. Diakow, P.A.; Thomas, J.K.; Vivanco, E.; Rodriguez, O. Fireball and flame venting comparisons: Test data, CFD simulations, and industry standard prediction. *J. Loss Prev. Process Ind.* **2022**, *77*, 104794. [CrossRef]
52. Sheng, Z.; Yang, G.; Li, S.; Shen, Q.; Sun, H.; Jiang, Z.; Liao, J.; Wang, H. Modeling of turbulent deflagration behaviors of premixed hydrogen-air in closed space with obstacles. *Process Saf. Environ. Prot.* **2022**, *161*, 506–519. [CrossRef]
53. Li, H.; Rui, S.; Guo, J.; Sun, X.; Li, G.; Zhang, J. Effect of ignition position on vented hydrogen–air deflagration in a 1 m^3 vessel. *J. Loss Prev. Process Ind.* **2019**, *62*, 103944. [CrossRef]
54. Lucas, M.; Hisken, H.; Skjold, T.; Arntzen, B.J.; van Wingerden, K. CFD modelling of hydrogen and hydrogen-methane explosions—Analysis of varying concentration and reduced oxygen atmospheres. *J. Loss Prev. Process Ind.* **2023**, *83*, 105012. [CrossRef]
55. Rui, S.; Wang, C.; Wan, Y.; Luo, X.; Zhang, Z.; Li, Q. Experimental study of end-vented hydrogen deflagrations in a 40-foot container. *Int. J. Hydrogen Energy* **2020**, *45*, 15710–15719. [CrossRef]
56. Duan, Y.; Yang, Y.; Deng, L.; Duan, X.; Qiao, Y.; Si, R. Influence of double explosion vent on methane-hydrogen explosion characteristics in confined space. *Fuel* **2026**, *407*, 137398. [CrossRef]

57. Wang, X.; Wang, C.; Fan, X.; Guo, F.; Zhang, Z. Effects of hydrogen concentration and film thickness on the vented explosion in a small obstructed rectangular container. *Int. J. Hydrogen Energy* **2019**, *44*, 22752–22759. [CrossRef]
58. Bang, B.H.; Ahn, C.S.; Lee, J.G.; Kim, Y.T.; Lee, M.H.; Horn, B.; Malik, D.; Thomas, K.; James, S.C.; Yarin, A.L.; et al. Theoretical, numerical, and experimental investigation of pressure rise due to deflagration in confined spaces. *Int. J. Therm. Sci.* **2017**, *120*, 469–480. [CrossRef]
59. Hu, Q.; Zhang, X.; Li, Q.; Hao, H.; Coffey, C.; Mitchell-Corbett, F. Prediction and interpretability of accidental explosion loads from hydrogen-air mixtures using CFD and artificial neural network method. *Int. J. Hydrogen Energy* **2024**, *66*, 135–147. [CrossRef]
60. Wu, Z.; Zhuang, Y.; Guo, J. Effects of hydrogen concentration on flame propagation and pressure evolution during vented H_2/air explosions in a vessel with a hinged panel. *Int. J. Hydrogen Energy* **2025**, *128*, 1–9. [CrossRef]
61. Li, Y.; Bi, M.; Zhang, S.; Jiang, H.; Gan, B.; Gao, W. Dynamic couplings of hydrogen/air flame morphology and explosion pressure evolution in the spherical chamber. *Int. J. Hydrogen Energy* **2018**, *43*, 2503–2513. [CrossRef]
62. Katsumi, T.; Aida, T.; Aiba, K.; Kadowaki, S. Outward propagation velocity and acceleration characteristics in hydrogen-air deflagration. *Int. J. Hydrogen Energy* **2017**, *42*, 7360–7365. [CrossRef]
63. Brzezińska, D. Hydrogen dispersion phenomenon in nominally closed spaces. *Int. J. Hydrogen Energy* **2021**, *46*, 28358–28365. [CrossRef]
64. Chen, Y.; Li, Z.; Ji, C.; Liu, X. Effects of hydrogen concentration, non-homogenous mixtures and obstacles on vented deflagrations of hydrogen-air mixtures in a 27 m^3 chamber. *Int. J. Hydrogen Energy* **2020**, *45*, 7199–7209. [CrossRef]
65. Rui, S.; Xiao, J.; Wang, F.; Kuznetsov, M.; Jordan, T. Numerical study of maximum overpressure in vented hydrogen explosions. *Process Saf. Environ. Prot.* **2025**, *200*, 107387. [CrossRef]
66. Rocourt, X.; Awamat, S.; Sochet, I.; Jallais, S. Vented hydrogen-air deflagration in a small enclosed volume. *Int. J. Hydrogen Energy* **2014**, *39*, 20462–20466. [CrossRef]
67. Zhang, X.; Chen, Y.; Ma, T.; Xu, Z.; Zhang, Y.; Xie, J.; Chen, J.; Zhou, X.; Shi, X.; Cao, W. Effect of ignition positions on hydrogen explosion venting characteristics: Flame structure, overpressure evolution, and flow field features. *Int. J. Hydrogen Energy* **2025**, *167*, 150983. [CrossRef]
68. Xu, J.; Chen, X.; Jiang, H.; Gao, W. Vented hydrogen-air explosions at elevated static activation pressures. *Process Saf. Environ. Prot.* **2022**, *168*, 474–486. [CrossRef]
69. Shi, J.; Li, J.; Hao, H.; Zhu, Y.; Chen, G. An integrated model for vent area design of hydrocarbon-air mixture explosion inside cubic enclosures with obstacles. *J. Loss Prev. Process Ind.* **2019**, *57*, 61–72. [CrossRef]
70. Ji, W.; Yu, J.; Yu, X.; Hou, Y.; Yan, X. Explosion venting of hybrid mixtures: A comparison of standards NFPA 68 and EN 14491. *J. Loss Prev. Process Ind.* **2018**, *54*, 325–332. [CrossRef]
71. Zheng, G.; Bai, Q.; Cheng, J.; Li, Y.; Gao, W. Study on hydrogen-air explosion flameless venting with metal foam addition. *Int. J. Hydrogen Energy* **2025**, *117*, 215–227. [CrossRef]
72. Zhang, S.; Tang, Z.; Li, J.; Wang, J.; Zhang, J.; Guo, J.; Li, Q. Effects of equivalence ratio, thickness of rupture membrane and vent area on vented hydrogen–air deflagrations in an end-vented duct with an obstacle. *Int. J. Hydrogen Energy* **2019**, *44*, 26100–26108. [CrossRef]
73. Guo, J.; Li, Q.; Chen, D.; Hu, K.; Shao, K.; Guo, C.; Wang, C. Effect of burst pressure on vented hydrogen-air explosion in a cylindrical vessel. *Int. J. Hydrogen Energy* **2015**, *40*, 6478–6486. [CrossRef]
74. Tang, Z.; Li, J.; Guo, J.; Zhang, S.; Duan, Z. Effect of vent size on explosion overpressure and flame behavior during vented hydrogen–air mixture deflagrations. *Nucl. Eng. Des.* **2020**, *361*, 110578. [CrossRef]
75. Pang, L.; Wang, C.; Han, M.; Xu, Z. A study on the characteristics of the deflagration of hydrogen-air mixture under the effect of a mesh aluminum alloy. *J. Hazard. Mater.* **2015**, *299*, 174–180. [CrossRef] [PubMed]
76. Vyazmina, E.; Jallais, S.; Krumenacker, L.; Tripathi, A.; Mahon, A.; Commanay, J.; Kudriakov, S.; Studer, E.; Vuillez, T.; Rosset, F. Vented explosion of hydrogen/air mixture: An intercomparison benchmark exercise. *Int. J. Hydrogen Energy* **2019**, *44*, 8914–8926. [CrossRef]
77. GEXCON. *FLACS-CFD v25.3 User's Manual*; GEXCON: Bergen, Norway, 2025.
78. Liang, Y.; Pan, X.; Zhang, C.; Xie, B.; Liu, S. The simulation and analysis of leakage and explosion at a renewable hydrogen refuelling station. *Int. J. Hydrogen Energy* **2019**, *44*, 22608–22619. [CrossRef]
79. Song, B.; Wang, X.; Kang, Y.; Li, H.; Li, M.; Cheng, Z. Hydrogen fuel cell vehicles on highways: Leakage diffusion characteristics and safety assessment. *Process Saf. Environ. Prot.* **2025**, *199*, 107255. [CrossRef]
80. Skjold, T.; Hisken, H.; Lakshmipathy, S.; Atanga, G.; Bernard, L.; van Wingerden, M.; Olsen, K.L.; Holme, M.N.; Turøy, N.M.; Mykleby, M.; et al. Vented hydrogen deflagrations in containers: Effect of congestion for homogeneous and inhomogeneous mixtures. *Int. J. Hydrogen Energy* **2019**, *44*, 8819–8832. [CrossRef]
81. Skjold, T.; Hisken, H.; Lakshmipathy, S.; Atanga, G.; Carcassi, M.; Schiavetti, M.; Stewart, J.R.; Newton, A.; Hoyes, J.R.; Tolias, I.C.; et al. Blind-prediction: Estimating the consequences of vented hydrogen deflagrations for homogeneous mixtures in 20-foot ISO containers. *Int. J. Hydrogen Energy* **2019**, *44*, 8997–9008. [CrossRef]

82. Baraldi, D.; Melideo, D.; Kotchourko, A.; Ren, K.; Yanez, J.; Jedicke, O.; Giannissi, S.G.; Tolias, I.C.; Venetsanos, A.G.; Keenan, J.; et al. Development of a model evaluation protocol for CFD analysis of hydrogen safety issues the SUSANA project. *Int. J. Hydrogen Energy* **2017**, *42*, 7633–7643. [CrossRef]
83. Hu, Q.; Zhang, X.; Hao, H. A review of hydrogen-air cloud explosions: The fundamentals, overpressure prediction methods, and influencing factors. *Int. J. Hydrogen Energy* **2023**, *48*, 13705–13730. [CrossRef]
84. Wang, Q.; Rui, S.; Wang, C. Improvement of engineering model for vented hydrogen explosion. *Int. J. Hydrogen Energy* **2024**, *83*, 89–98. [CrossRef]
85. Makarov, D.; Verbecke, F.; Molkov, V.; Kotchourko, A.; Lelyakin, A.; Yanez, J.; Baraldi, D.; Heitsch, M.; Efimenko, A.; Gavrikov, A. An intercomparison of CFD models to predict lean and non-uniform hydrogen mixture explosions. *Int. J. Hydrogen Energy* **2010**, *35*, 5754–5762. [CrossRef]
86. Cao, W.; Zhou, Z.; Zhou, W.; Xu, S.; Xiao, Q.; Cao, W.; Jiao, F.; Zhang, Y.; Yu, S.; Xu, S. The flow field behaviours of under-expansion jet flame in premixed hydrogen/air explosion venting. *Int. J. Hydrogen Energy* **2022**, *47*, 10420–10430. [CrossRef]
87. Tolias, I.C.; Stewart, J.R.; Newton, A.; Keenan, J.; Makarov, D.; Hoyes, J.R.; Molkov, V.; Venetsanos, A.G. Numerical simulations of vented hydrogen deflagration in a medium-scale enclosure. *J. Loss Prev. Process Ind.* **2018**, *52*, 125–139. [CrossRef]
88. Hisken, H.; Atanga, G.; Skjold, T.; Lakshmipathy, S.; Middha, P. Validating, documenting and qualifying models used for consequence assessment of hydrogen explosion scenarios. In Proceedings of the 11th International Symposium on Hazards, Prevention and Mitigation of Industrial Explosions ISHPMIE, Dalian, China, 24–29 July 2016.
89. García, J.; Baraldi, D.; Gallego, E.; Beccantini, A.; Crespo, A.; Hansen, O.R.; Høiset, S.; Kotchourko, A.; Makarov, D.; Migoya, E.; et al. An intercomparison exercise on the capabilities of CFD models to reproduce a large-scale hydrogen deflagration in open atmosphere. *Int. J. Hydrogen Energy* **2010**, *35*, 4435–4444. [CrossRef]
90. Diakow, P.A.; Thomas, J.K.; Vivanco, E. Comparison of large-scale vented deflagration tests to CFD simulations for partially congested enclosures. *J. Loss Prev. Process Ind.* **2018**, *56*, 147–154. [CrossRef]
91. Grégoire, Y.; Daubech, J.; Proust, C.; Leprette, E. Vented gas explosion overpressure calculation based on a multi-layered neural network. *J. Loss Prev. Process Ind.* **2022**, *74*, 104641. [CrossRef]
92. Xu, Q.; Chen, G.; Su, S.; Men, J.; Li, G. Prediction of venting gas explosion overpressure based on a combination of explosive theory and machine learning. *Expert Syst. Appl.* **2023**, *234*, 121044. [CrossRef]
93. Covoni, G.; Bisio, V.; Rossin, S.; Ruggiero, M.; Montomoli, F.; Tagarielli, V.L. Predictions of realistic hydrogen deflagrations with graph neural networks. *Int. J. Hydrogen Energy* **2026**, *225*, 154343. [CrossRef]
94. Sinha, A.; Rao, V.C.M.; Wen, J.X. Performance evaluation of empirical models for vented lean hydrogen explosions. *Int. J. Hydrogen Energy* **2019**, *44*, 8711–8726. [CrossRef]
95. Hu, Q.; Zhang, X.; Hao, H. Prediction of peak overpressure from hydrogen-air cloud explosions in vented cylindrical vessels. *Process Saf. Environ. Prot.* **2024**, *190*, 1093–1104. [CrossRef]
96. Tolias, I.C.; Venetsanos, A.G. An improved CFD model for vented deflagration simulations—Analysis of a medium-scale hydrogen experiment. *Int. J. Hydrogen Energy* **2018**, *43*, 23568–23584. [CrossRef]
97. *EN 14994:2007*; Gas Explosion Venting Protective Systems. European Committee for Standardization: Brussels, Belgium, 2007.
98. National Fire Protection Association. *NFPA 68: Standard on Explosion Protection by Deflagration Venting*, 2023rd ed.; National Fire Protection Association: Quincy, MA, USA, 2023.
99. European Parliament; Council of the European Union. Directive 1999/92/EC of the European Parliament and of the Council of 16 December 1999 on Minimum Requirements for Improving the Safety and Health Protection of Workers Potentially at Risk from Explosive Atmospheres. *Off. J. Eur. Communities* **2000**, *L 23*, 57–64.
100. European Parliament; Council of the European Union. Directive 2014/34/EU of the European Parliament and of the Council of 26 February 2014 on the Harmonisation of the Laws of the Member States Relating to Equipment and Protective Systems Intended for Use in Potentially Explosive Atmospheres. *Off. J. Eur. Union* **2014**, *L 96*, 309–356.
101. *EN 14797:2006*; Explosion Venting Devices. European Committee for Standardization: Brussels, Belgium, 2006.
102. *EN 14460:2018*; Explosion Resistant Equipment. European Committee for Standardization: Brussels, Belgium, 2018.
103. *EN 1127-1:2019*; Explosive Atmospheres—Explosion Prevention and Protection—Part 1: Basic Concepts and Methodology. European Committee for Standardization: Brussels, Belgium, 2019.
104. National Fire Protection Association. *NFPA 2: Hydrogen Technologies Code*, 2026th ed.; National Fire Protection Association: Quincy, MA, USA, 2026.
105. *ISO/TS 15916:2026*; Hydrogen Technologies—Basic Considerations for the Safety of Hydrogen Systems. International Organization for Standardization: Geneva, Switzerland, 2026.